Immobilization of Cutinase on Nanoparticles

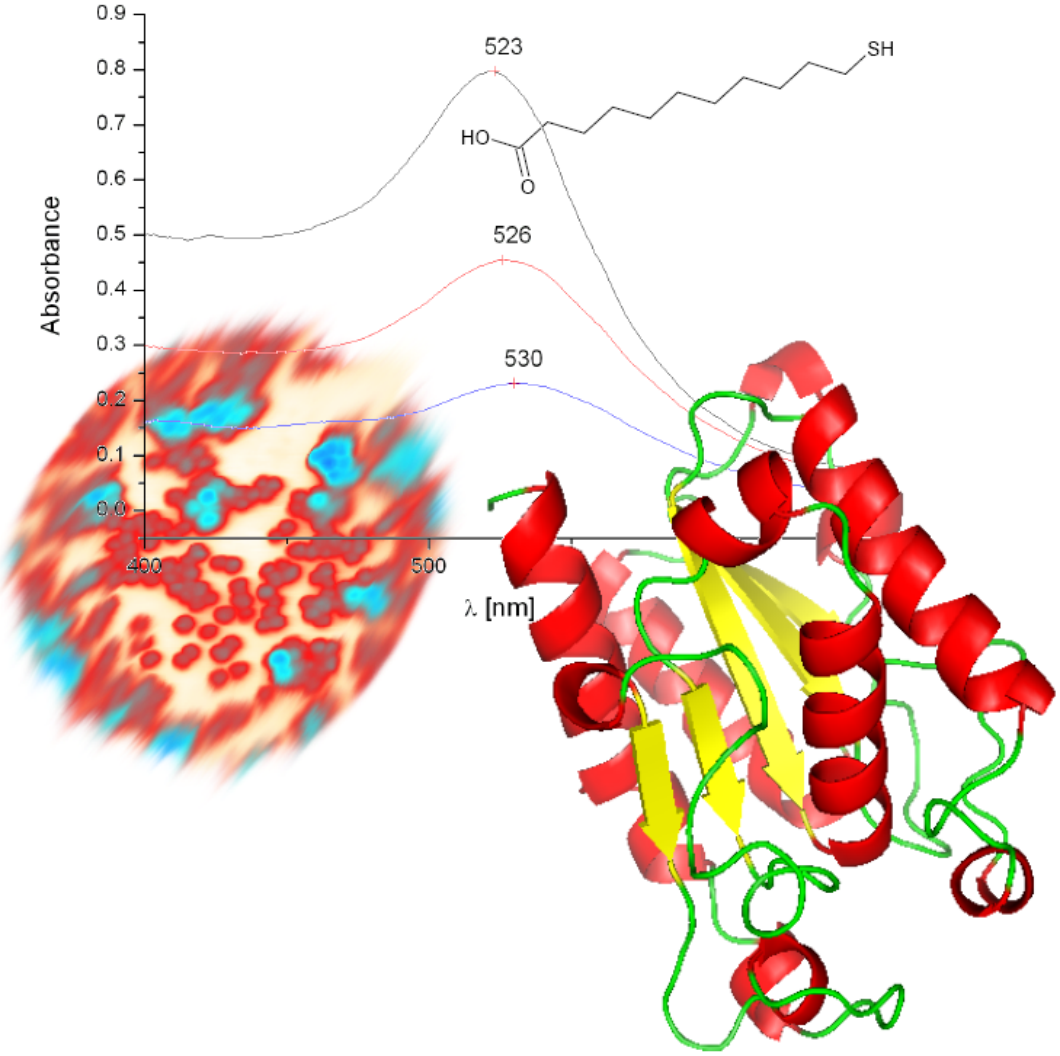

A Project by 5th Semester Nanotechnology Students

Project Group N544

AALBORG UNIVERSITY
FACULTY OF PHYSICS AND NANOTECHNOLOGY

Skjernvej 4C ▪ DK-9220 Aalborg Øst

Title: Immobilization of Cutinase on Nanoparticles
Project Period: 4th of September 2006 - 21th of December 2006
Project Group: N544

Synopsis

This project focuses on the *immobilization of proteins on gold and polystyrene nanoparticles*. Gold nanoparticles at around 14 nm in diameter were produced by reduction of $HAuCl_4$ in the presence of the stabilizing agent trisodium citrate. Polystyrene nanoparticles at 40 nm and 510 nm were purchased. Immobilization on gold particles was done by first attaching a linker on the gold particles and finally attaching the protein on the linkers. 16-MHDA and 11-MUDA linkers activated by EDC and NHS were tried. The polystyrene particles already had linkers on the surface and was thus easier to work with. Cutinase was used as the protein. Characterization of the particles by DLS, AFM, CD and Absorbance Spectroscopy was made after and during the immobilization process. Finally the kinetics of the immobilized proteins was studied. The results when using 16-MHDA was better than those when using 11-MUDA. The best results were obtained from the 510 nm polystyrene particles. The immobilization on the 40 nm polystyrene particles did not succeed. Only one pro mille of the enzymes were retained on the nanoparticles, which is not satisfactory when considering costs.

Project group:
René Petersen
Tom Larsen
Ole Z. Andersen
Nikolaj L. Kildeby

Contact:
aauprojects@repetit.dk

Supervisor:
Peter Fojan
Leonid Gurevich

Circulation: 8
Number Of Pages: 71
Finished: 21th of December 2006

Preface

This report is the product of the 5th semester project period on the nanotechnology education on Aalborg University, Denmark.
The report is addressed to people with an interest in immobilization of proteins for production a nanoparticle based biosensors and with a basic knowledge in the experimental methods AFM, LSPR based Absorbance Spectroscopy and DLS and the theoretical fields of enzyme kinetics and surface plasmon resonance.
The report has been typeset in LaTeX2e.

Structure of The Report

The report is divided into chapters, sections and subsections. The first chapter, "Introduction" gives a basic knowledge of biosensors generally and immobilization of proteins on nanoparticles. The chapter "Theoretical Foundation" describes the theory which is essential for a good understanding and interpretation of the results obtained. Materials and Methods describes the experimental part of the project. The "Results" chapter is the part of the report where the obtained results are presented. The "Discussion" chapter summarizes discusses the results in relation to each other. In the "Conclusion" chapter conclusions on the results will be made. Finally, a number of appendices are present in the last part of the report.

Instructions For Reading

It is expected that sections in each chapter are read together and that the chapters are read in their chronological order.
The notation used to references is the Harvard method and these are listed in alphabetic order in the bibliography, in the back of the report.
Figures and tables are numbered sequentially in each chapter.

CONTENTS

CHAPTER 1

Introduction

1.1 Biosensors

Sensors of different types are frequently used in areas like food, pharmaceutical, chemical industries, environment surveillance, defense, and security. This constant use of sensors makes it attractive to develop new sensors which are simpler, cheaper and more precise.

Since the term sensor covers a wide variety of devices it is appropriate with a clear definition of the term. According to Oxford English Dictionary a sensor is defined as a device that detects or measures a physical property and records, indicates or otherwise responds to it.[Catherine Soanes et al., 2006] Since this definition is wide, the term is often divided into three classes namely physical, chemical, and biological sensors. Physical sensors are used to measure distance, mass, temperature, pressure, etc. A chemical sensor is a device which responds to a particular analyte in a selective way through a chemical reaction. Biosensors measure chemical substances by using a biological sensing element. Physical and chemical sensors will not be treated any further in this report.[Eggins, 2006]

A biosensor consists of three main parts, as illustrated in Figure 1.1: Firstly, a recognition element which is the part of the sensor that makes it able to respond to a particular analyte or groups of analytes. The recognition element in biosensors is always a biological species and enzymes, antibodies, nucleic acids etc. are commonly used. Secondly, a transducer which connects the recognition element to the signal processing system. The transducer transforms the molecular absorption and/or the chemical reaction into some kind of response like an electrical-, optical-, thermal-, or mechanical response. Lastly, a signal processing system which displays the measurable response in a suitable form.[Eggins, 2006]

A wide variety of designs are used in the construction of biosensors and that makes this field a multidisciplinary field involving biochemistry, physical chemistry,

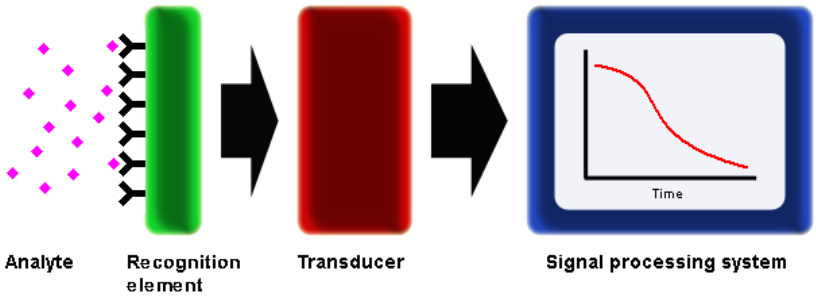

Figure 1.1: Schematic illustration of a biosensor

electrochemistry, electronics and software engineering. Common for all these different designs is that they have to fulfill some of the following features before they can be considered as a successful design. The recognition element has to be highly specific for the purpose of the analyses. The response has to be accurate and precise, which means better than ±5%. It is also important that the response is reproducible. It should be possible to perform the analyses without any pre-treatment of the sample. The biosensor must be stable under normal conditions in order to make the working lifetime as long as possible. The response and recovery time has to be as short as possible. Response and recovery time is often longer for biosensors than for chemical sensors, typically 30 seconds or more. If the biosensor is for use in clinical situations is it important for the probe to be biocompatible, having no toxic or antigenic effects. In this relations it could be necessary that the probe is sterilisable, which is a problem since the recognition element is made of biological species.[Eggins, 2006].

1.2 Immobilization

The immobilization process is often a necessity within areas that involves the attachment of an active element such as biosensors or enzymes used to catalyze an industrial reaction.

In the case of biosensors immobilization is often carried out to attach the active element to for example an electrode or to the surface of specific area of the sensor construct.

In relation with the industrial field a number of enzyme reactors has been developed. The way these reactors work are diverse; some work by simply adding enzyme to the substrate and then stirring. These are called stirred tank batch reactors (STR). The disadvantage of such a tank is that the enzyme cannot be recycled and new enzymes must therefore be added after each cycle. Here the immobilization can be used to ensure that the enzymes can be reused a number of times. Such an immobilization can for instance be carried out so that the enzymes are deployed

on the surface of the tank. This however will cause the reactive surface/volume area to drop thereby increasing the reaction time and making the stirring even more important. [www.lsbu.ac.uk, 2006]

Another reactor that utilizes the immobilization is the fluidized bed reactor (FBR). Here the enzymes are immobilized on granules that are kept suspended by gas or substrate flow. This increases the surface area and accelerates the reaction. The granules are easily collected and replaced [www.lsbu.ac.uk, 2006]. These granules can be exchanged with for example gold nanoparticles for further increase of the reactive surface of the reactor. The separation of the particles can be achieved using a cyclone separator. This however sets a lower limit for the particle size and density.

1.3 Project Description

The use of biosensors is in a growing stage as more and more possibilities are explored with modern science. Protein immobilization on gold nanoparticles or surfaces is an already known and studied biosensor concept as it makes it possible to reuse the proteins. In this project this concept is further studied and optimized. Immobilization techniques on gold nanoparticles will be optimized using 2 different linkers, 11-mercaptoundecanoic acid and 16-mercaptohexadecanoic acid, with carboxyl groups. The size distribution of gold nanoparticles will be characterized using DLS and AFM.

Polystyrene nanoparticles of different sizes will also be used in order to see if they provide a better result than gold. These however already have carboxyl groups attached to the surface.

The studies will be conducted using the enzyme cutinase as the immobilized protein. The enzyme activity will be measured with absorbance spectroscopy. Absorbance spectroscopy will also be used to measure LSPR for gold nanoparticles.

1.3.1 Problem Statement

The aim of the project is to answer the following questions:

- How can enzymes be effectively immobilized onto nanoparticles?
- How can the activity of the immobilized enzymes be studied?
- Does the presence of the nanoparticle inhibit or destroy the enzyme?

CHAPTER 2

Theoretical Foundation

2.1 Gold Nanoparticles

This section will describe the relevant properties of gold nanoparticles concerning the immobilization of proteins. In this regard the synthesis of gold nanoparticles will be described.

The use of colloidal gold can be dated back to ancient times where it was used in stained glass. Since then a lot have been learned about gold nanoparticles and they have proven useful in a wide variety of applications within areas of nanotechnology, including electronics, medicine and biosensors. The possibility of modifying the surface of gold is especially interesting within the field of biosensors. Furthermore, the preparation of colloidal gold is cheap and does not require expensive equipment or highly educated staff. This also makes colloidal gold attractive in the research and devolvement of new and more advanced biosensors.

2.1.1 Gold Nanoparticles in Biosensors

It is a well known fact that colloids in general possess a high surface to volume ratio and this also applies to gold nanoparticles. This is interesting in regard to direct electron transfer between redox proteins and an electrode surface. The high surface energy and high surface to volume ratio of gold nanoparticles facilitate the electron transfer between immobilized proteins and electron surface without the use of an electron-transfer mediator, which will make it possible to build a mediator free sensor. [S. Liu et al., 2003]

The stability of the surface of gold nanoparticles is a more interesting aspect in relation to the biosensor concept based on immobilization of proteins. Gold nanoparticles have played a more and more important role in the biosensor research over the last years because of their ability to provide a stable surface for the immobilization of

biomolecules using linkers. One advantage of using immobilized biomolecules is that they can be reused but this can sometimes be at the expense of a weaker biological activity. This disadvantage can however be resolved by using a larger concentration of immobilized biomolecules. [S. Liu et al., 2003]

2.1.2 Synthesis of Gold Nanoparticles

As already mentioned stable nanoparticles are important in order to achieve the above properties. These are normally produced by reducing gold ions into solid gold. This can be done by using hydrogen tetrachloroaurate ($HAuCl_4$) as source of gold ions and trisodium citrate ($Na_3C_6H_5O_7$) as reduction agent. The flowchart of this reaction is shown in Equation 2.1, Equation 2.2 and Equation 2.3. The flowchart is only balanced with respect to gold. [www.fu berlin.de, 2006]

$$\mathrm{Na_3C_6H_5O_7} \xrightarrow{\mathrm{H_2O}} \mathrm{C_6H_5O_7^{3-}} + 3\,\mathrm{Na^{3+}} \tag{2.1}$$

$$3\,\mathrm{C_6H_5O_7^{3-}} + 2\,\mathrm{Au^{3+}} \longrightarrow 2\,\mathrm{Au} + 3\,\mathrm{C_5H_4O_5^{2-}} + 3\,\mathrm{CO_2} \tag{2.2}$$

$$3\,\mathrm{C_5H_4O_5^{2-}} + 16\,\mathrm{Au^{3+}} \longrightarrow 16\,\mathrm{Au} + 15\,\mathrm{CO_2} \tag{2.3}$$

As the gold ions are reduced to neutral gold atoms they precipitate from the solution and form gold aggregates that grow in size until no more gold is available. These aggregates or nanoparticles are stabilized by the remaining citrate molecules as they settle on the particle surface making them appear negatively charged. The particles are thereby stabilized through electrostatic repulsion. Figure 2.1 illustrates how citrate stabilizes the nanoparticles. The size of the produced particles can be controlled to a certain extent by varying the amount of available gold ions in the solution.

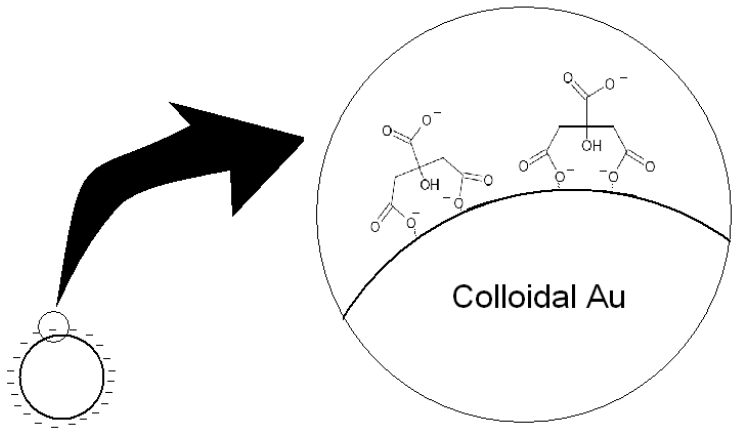

Figure 2.1: A citrate stabilized gold particle.

2.2 Polystyrene Nanoparticles

Polystyrene was discovered in 1839 by Eduard Simonis. It is a polymer made from the toxic monomer styrene. An illustration of mono- and polymer can be found in Figure 2.2.

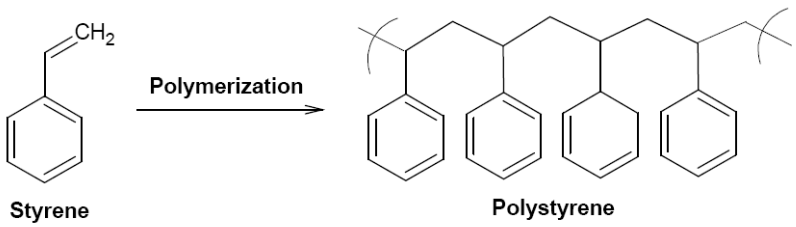

Figure 2.2: The monomer styrene and the polymer polystyrene

While styrene is an oily liquid at room temperature, polystyrene is a solid. Polystyrene is a common product in science and especially biology as petri dishes, test tubes and similar are made from polystyrene. [www.wikipedia.org/Polystyrene, 2006]

Polystyrene nanoparticles are commercially available in a wide range of sizes with narrow size distributions. They have become a widely used material as they can be purchased surfactant-free as well as modified with various surfactants, such as linkers, dyes, biomolecules, and covalently bound functional groups. Working with these particles can therefore save a great amount of time when used for immobilization of biomolecules compared to metal nanoparticles where linkers first have to be attached. This great variety causes polystyrene nanoparticles to be used in a wide range of areas within nanotechnology. They are for instance used in the field of biosensors where they serve as labels, sensing probes and carriers of biomolecules. [M. Himmelhaus and TH. Takei, 2002]

2.3 Immobilization of Enzymes

This section will focus on the chemistry of the immobilization process. Starting with a description of the linkers used, then explaining how these are attached to the gold surface, and ending with the procedure of the actual immobilization.

2.3.1 Linkers

In order to attach the proteins to the citrate stabilized gold particles mercaptoalkane linkers are used. These are 11-mercaptoundecanoic acid and 16-mercaptohexadecanoic acid where the number denotes the position of the mercapto group in relation to the carboxyl group. An illustration of the two linkers used in this project can be found in Figure 2.3. [K. Aslan and V. H. Pérez-Luna, 2002]

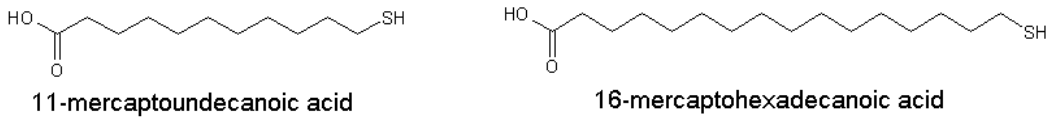

Figure 2.3: The linkers used to attach proteins to the gold particles. The only difference between the two mercaptoalkanes illustrated is the number of atoms in the carbon chain. Both molecules has a thiol group and a carboxyl group at the right and the left end respectively.

The linkers replace the citrate molecules but if the particles are not stabilized under the substitution they will aggregate. This aggregation will happen as the nanoparticles try minimizing their surface energy by clustering together. To deal with this Tween 20 is introduced into the solution and is adsorbed onto the surface of the particles and at the same time forcing the citrate molecules away from the surface. When the mercaptoalkanes are introduced they form a monolayer on the particle surface while the Tween 20 shields the reaction. Figure 2.4 illustrates the function of Tween 20. [K. Aslan and V. H. Pérez-Luna, 2002]

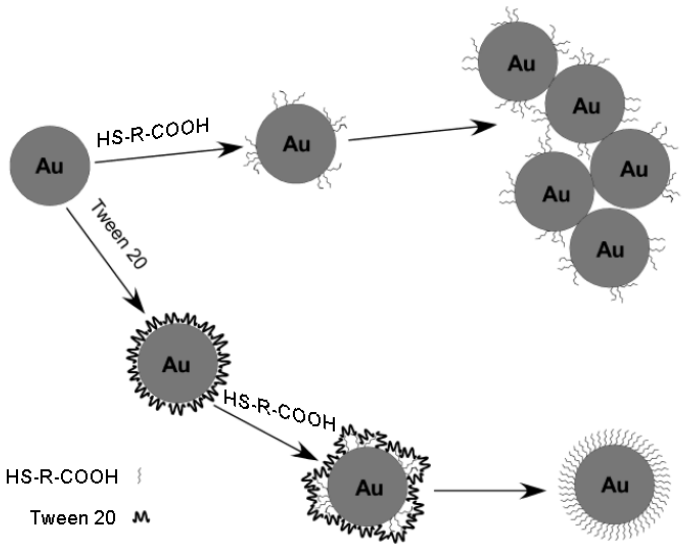

Figure 2.4: Illustrates the function of Tween 20. If Tween 20 is not added to the solution the particles will aggregate. Modified from [K. Aslan and V. H. Pérez-Luna, 2002]

The thiol group of the mercaptoalkanes interact with the gold surface through an $Au - S$ interaction. The strength of this bond is on the order of 40 kcal/mole.

2.3.2 Thiol Chemistry

Thiols are organic compounds which contain the functional group -SH. This functional group is referred to as a thiol group or a sulfhydryl group. Compounds

containing thiol groups are also sometimes referred to as mercaptans.

Thiols can be viewed as the sulfur analog of alcohols. Alcohols are organic compounds containing an -OH group. In thiols the oxygen atom has been replaced by a sulfur atom. Because oxygen and sulfur both belong to group number six of the periodic table, alcohols and thiols share some common chemical properties. However, because of the small electronegativity difference between hydrogen and sulfur (ΔEN=0.38) the covalent SH bond is practically non-polar. This results in a decreased tendency of thiols to form hydrogen bonds, compared to that of alcohols. Therefore, the boiling point of thiols is often lower then the boiling point of the corresponding alcohol.[www.wikipedia.org/Thiol, 2006]

2.3.3 Stability and Strength of Linker/Au Interaction

The strength of the bond between the linker and the Au gold particle is of great importance for the functionality of the biosensor. If the bond is too weak it could break under certain circumstances, for example in certain solutions, under exposure to light or exposure to high temperatures. One has to be aware of these limitations in order to ensure correct usage and function of the sensor.

The strength of the Au-S bond is, as given in Section 2.3.2, 40 kcal/mol. This value can be used to estimate the bond-strength per molecule. Using 1 kcal = 4184 J and 1 eV = 1.602×10^{-19} J together with Avogadros Number, $N_A = 6.022 \times 10^{23}$ gives a strength per molecule of 1.73 eV.

This calculation gives the bond strength per linker molecule. In comparison, the energy of photons from the visible light spectrum (400-700) ranges from 1.77 eV to 3.10 eV. Thus, theoretically, visible light would be able to break the Au-S bond. In practice however, this does not happen due to a further interaction between the closely spaced linkers. Due to the length of the linkers the Van der Waals interaction between adjacent linker molecules acts to keep the molecules near the gold surface long time enough for the Au-S bond to reform. If the linker molecules where short, the interaction would not be as strong and it would be easier to knock off the linkers. In addition to this interaction between adjacent linker molecules, the end of the linkers pointing towards the Au gold particles is hydrophobic, which also prevents the linker from getting knocked off the gold particle and into the solution.

As for the temperature, the thermal energy k_BT at room temperature is on the order of 0.025 eV, far too small to break the Au-S bond. This means that the temperature should not be a concern when it comes to the stability of the gold/linker complex.

2.3.4 Immobilization

The particles are now ready for the attachment of proteins as the particles are now stabilized by a monolayer of mercaptoalkanes with the carboxyl group facing the solvent. The immobilization happens through the primary amines of the proteins and the carboxyl groups of the linkers. The carboxyl groups need to be activated

before they can react with the amino groups. The activation is carried out by using 1-Ethyl-3-(3-dimethylaminopropyl)-carbodiimid (EDC) and N-Hydroxysuccinimide (NHS). The treatment with EDC will activate the carboxyl groups but the result is an unstable compound that requires the proteins to be in the solution while the activation takes place. If they do not react the modified carboxyl groups will hydrolyze back to their previous state [D. M. Schulz and A. Sinz, 2004]. The enzymes also have carboxyl groups on the surface and if these are activated by EDC they will cause the whole construct to aggregate as the proteins would function as a link between the nanoparticles.

To prevent aggregation in the solution NHS is used. NHS reacts with the EDC activated groups in order to create a semi-stable amine reactive NHS-ester [D. M. Schulz and A. Sinz, 2004]. Now the proteins can be introduced and they will be immobilized at the end of the linker through the formation of an amide bond. A description of the treatment with EDC and NHS can be seen in Figure 2.5.

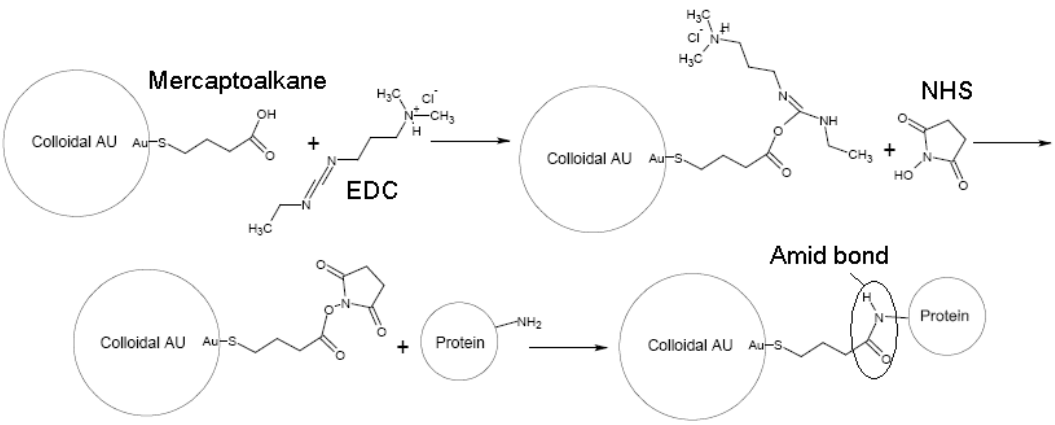

Figure 2.5: Illustration of EDC/NHS activation of carboxyl groups of the linker molecule and the reaction of the activated linker with an amino group of a protein. Modified from [www.piercenet.com, 2006]

2.4 Surface Plasmon Resonance (SPR)

In this section the phenomena of SPR and its applications to biochemistry and biosensors will be described. First a brief introduction to the physics behind surface plasmons is given. What is a plasmon, how can it be created, and what materials support plasmons are some of the questions which will be answered. After the physical foundation has been established the impact that SPR has had on biochemistry is described. [Vadgama, 2005]

2.4.1 Physical Background

Plasmons are collective excitations of the electron gas at optical frequencies. One can imagine a plasmon as a collective displacement of the electron cloud with respect to the fixed ions (assuming ions of infinite mass). The coulomb interaction between the displaced electrons and the fixed ions will act as a restoring force, acting to restore the original electron configuration. The electrons will thus be oscillating, and the frequency of oscillation is given by the plasma frequency, ω_p:

$$\omega_p = \sqrt{\frac{ne^2}{m_e \epsilon_0}} \tag{2.4}$$

Where n is the electron concentration, e is the electronic charge, m_e is the electron mass and ϵ_0 is the vacuum permittivity. Plasmons play an important role in the optical properties of matter. Light below the plasmon frequency is reflected because the electrons screen the electric field of the light. Light above the plasma frequency is transmitted because the electrons cannot respond fast enough to screen it. In most metals the plasma frequency lies in the ultraviolet giving them the shiny surface characteristic for metals. Other metals, like copper for example, have plasma frequencies in the visible range giving them their distinct color.

The plasma frequency of gold lies in the ultraviolet range, but geometrical factors come into play when the particles become small, shifting the plasma frequency into the visible range.

Surface plasmons are oscillations of electrons at the surface of a bulk material. The kinetic energy of the electrons at the surface will cause some of them to move away from the bulk and this will in turn increase their potential energy and draw them back to the bulk again. This oscillation of electrons is termed a surface plasmon and is a transversal wave traveling on the surface of the particle. When surface plasmons are excited on nanometer sized structures they are called localized surface plasmons.

Surface plasmons can be excited by electromagnetic radiation if the frequency of the incoming light matches the frequency of the surface plasmons. To excite surface plasmons the light have to be polarized in the plane of incidence (perpendicular to the surface).

The dielectric material surrounding the metal influences the frequency of surface plasmons so that the frequency of a surface plasmon is given by:

$$\omega_{sp} = \frac{\omega_p}{\sqrt{1 + \epsilon_d}} \tag{2.5}$$

Where ω_{sp} is the frequency of the surface plasmons, and ϵ_d is the permittivity of the surrounding dielectric. The SPR phenomena can be detected as a characteristic peak in the absorbance spectrum of a material. A solution of gold nanoparticles for example, shows a peak at 520 nm due to the LSPR of the gold particles. [Kittel, 2005]

2.4.2 Application of LSPR to Bio/Chemical-Sensors

The phenomena of LSPR has become widely used in biochemistry because of its high sensitivity to changes in the local environment. It is evident from Equation 2.5 that it is changes near the surface which are decisive for the position of the lSPR peak, because the frequency of surface plasmons depends only on the dielectric constant of the surrounding media. If a change near the surface of a material supporting LSPR can be induced as a result of a chemical reaction or biological activity, this event can be detected by measuring changes in LSPR peak wavelength. To induce changes near the surface, the surface can be chemically tailored to bind certain key molecules which measures the degree of activity, or directly bind the molecules to sense for. The degree of shifting of the LSPR peak wavelength is thus a measure of the activity or molecular concentration respectively. [Kittel, 2005]

2.5 Determination of Protein Concentration

Measuring the protein concentration of a sample is not a trivial task. Measurements of the absorbance of the sample however, provides an easy way to determine the protein concentration *if* the molar absorbance coefficient is known, for then Lambert-Beers law can be applied, Equation 2.6

$$\epsilon lc = -Log_{10}\left(\frac{I_1}{I_0}\right) \tag{2.6}$$

Where ϵ is the molar absorption coefficient, l is the path length the light has to travel, c is the concentration of the sample and I_0 and I_1 is the intensity of incident light and light after passing through the sample. It is obvious that knowledge of ϵ would provide an easy key to determine the concentration, because all other unknowns are easily measurable. The problem however, often lies in correct determination of the molar absorbtion coefficient.

The molar absorption coefficient can be determined from knowledge of the protein structure. It is the amino acids tryptophan, tyrosine and cystine which determines the absorption of a protein at 280 nm. Therefore, if the molar absorption coefficient of these amino acids is known, the absorbance coefficient of the protein can be calculated. These coefficients are given in Equation 2.7 and from this equation the absorption coefficient of the protein at 280 nm can be calculated. [C. N. Pace et al., 1995]

$$\epsilon_{prot} = (\#Trp) \times 5500 + (\#Tyr) \times 1490 + (\#Cys) \times 125 \tag{2.7}$$

Where ϵ_{prot} is the molar absorption coefficient of the protein. $\#Trp$, $\#Tyr$ and $\#Cys$ is the number of tryptophan, tyrosine and cystine amino acids respectively. The constants are the absorbtion coefficients of the three amino acids. For cutinase the numbers of trp, tyr and cys are respectively 1, 6 and 2. This gives an ϵ_{prot} of 14690 M^{-1} cm^{-1}.

With knowledge of the absorption coefficient calculation of the concentration is trivial.

2.6 Cutinase

This section will describe the function and structure of the enzyme used in the immobilization process. The structure will be described using already analyzed cutinase from the RCSP Protein Data Bank using the PDB ID 1CEX.

2.6.1 Function of Cutinase

Cutinase is a part of the lipase family where a lipase generally is any enzyme capable of degrading lipid molecules by catalyzing the hydrolysis of ester bonds. It is for instance used in the breakdown of fats into absorbable forms. Cutinase is in nature used in the breakdown of cutin, a polymer used to protect plants against pathogens, but it is also used in industrial processes. It is used as detergents in laundry and dishwasning as a lipolytic enzyme to remove fat. Another area is in the degradation of plastics into water-soluble product. The activity of cutinase can be determined spectrophotometrically by measuring the hydrolysis of p-nitrophenylbutyrate (p-NPB). [G. A. Macedo and T. F. Pio, 2005]

2.6.2 Structure of Cutinase

Cutinase is a one-domain molecule with a size of 45x30x30 Å. It consist of 213 residues and has a molecular weight of 22,290 Da. The secondary structure consist of five parallel β-strands which form a β-sheet in the center and the β-sheet is covered by two and three α helices on each side, which is shown in Figure 2.6(a). The active site is located at Ser120, this is shown in Figure 2.6(b) along with the other catalytic residues, Asp175, and His188. All three are accessible to the solvent. [www.rcsb.org, 2006]

There are 6 Lysine (65, 108, 140, 151, 168, 206) and 13 Arginine (17, 20, 40, 78, 88, 96, 138, 156, 158, 166, 196, 208, 211) present. These amino acids have the primary amines which are used in binding with the linker as described in Section 2.3.4. Lysine are the most reactive residue and will therefore react strongest to the carboxyl groups. All residues are found to be exposed on the surface. Figure 2.6(c) shows the primary amines close to the active site. The only primary amines close to the active site is Arg40 and Arg78. Since the carboxyl groups will react strongest to the Lysine residues, the active site will therefore most likely be oriented away from the carriers (i.e. gold nanoparticles) and facing the solution.

Cutinase contains 1 trp, 6 tyr and 2 cys amino acid residues. These residues are responsible for most of the ultraviolet absorbance of the enzyme, with molar absorbance at 280 nm of 5500 $M^{-1}cm^{-1}$, 1490 $M^{-1}cm^{-1}$ and 125 $M^{-1}cm^{-1}$ respectively. [Creighton, 1993]

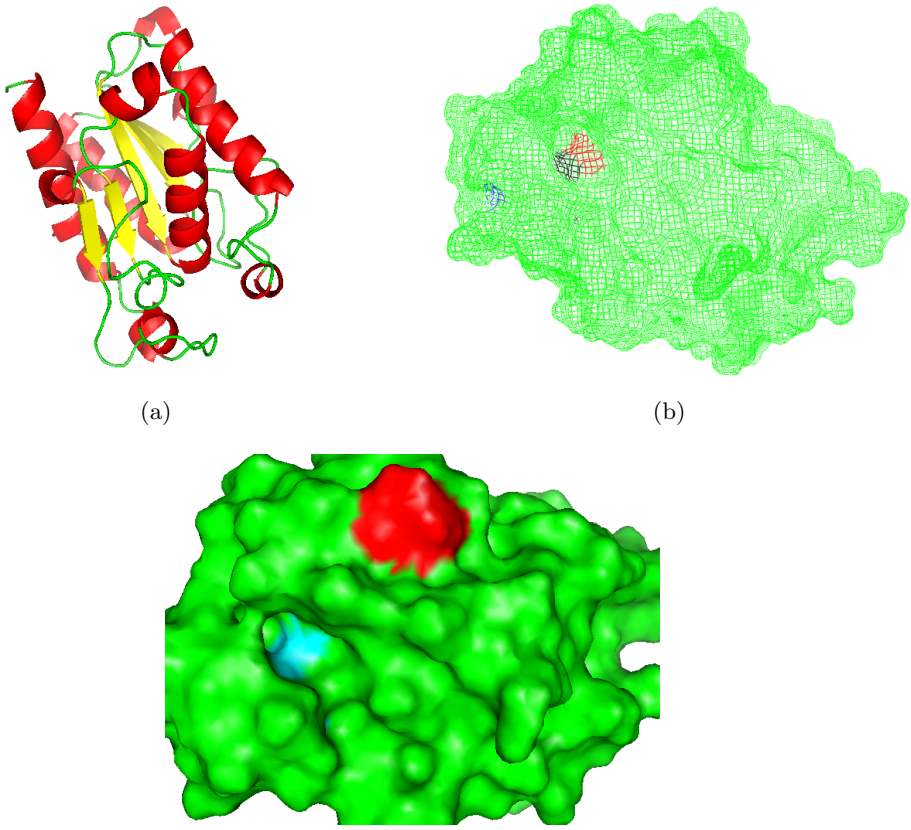

Figure 2.6: The secondary structure of Cutinase with PDB ID 1CEX. Figure 2.6(a) shows the β-sheet with α helices placed on each side. Figure 2.6(b) shows the active site of Cutinase. Ser120 is shown in red, Asp175 in blue, and His188 in black. Figure 2.6(c) shows the primary amines, Arg40 and Arg78 (both in red) close to the active site (cyan).

2.7 Enzyme Kinetics

Enzyme kinetics is the study of the reaction rate of an enzyme-catalyzed reaction. A kinetic analysis of enzyme-catalyzed reactions provide information about the specificities and catalytic mechanisms of the enzymes. This section will give an insight into the subject enzyme kinetics and thereby serves as a theoretical foundation for the activity assays, which will be carried out in the laboratory.

2.7.1 Kinetics

Kinetics experiments of enzyme-catalyzed reactions examine the relationship between the amounts of products produced per time and the conditions under which

the reactions take place. The velocity v of a reaction varies with the concentration of each reactant, whether enzymes are present or not. The rate equation for a nonenzymatic reaction of a substrate S to the product P can mathematically be expressed as in Equation 2.8.

$$\frac{\Delta[P]}{\Delta t} = v = k[S] \tag{2.8}$$

The squared brackets refer to the concentration of the product and the substrate. The constant k is the rate constant, which is a proportionality factor that describes the speed of a reaction. The rate constant is specific for any reactions.

A simple enzymatic reaction will be used to explain the general principles of enzyme kinetics. In the reaction a substrate S is converted to a product P. The reaction is catalyzed by an enzyme E.

When the reaction have been started it can in the beginning be symbolized as in Equation 2.9, since the amount of product produced can be neglected.

$$\mathrm{E} + \mathrm{S} \underset{\mathrm{k}_{-1}}{\overset{\mathrm{k}_1}{\rightleftharpoons}} \mathrm{ES} \xrightarrow{\mathrm{k}_{\mathrm{cat}}} \mathrm{E} + \mathrm{P} \tag{2.9}$$

The enzyme E and the substrate S combine and form an enzyme-substrate complex. The substrate reacts with the active site of the enzyme and forms the product of the reaction. The end of the equation is the product and the free enzyme, which can be used to catalyze a new reaction. The rate constants k and k_{-1} describe the rate of the association of S with E and the dissociation of S from the ES complex respectively. The rate constant k_{cat} is the catalytic constant or the turnover number, which describes the catalytic events per second per enzyme. As it can be seen in Equation 2.9 the conversion of enzyme-substrate complex into free enzyme and product is a one-way reaction. This assumption in only true in the initial period of the reaction, since the rate of the reverse reaction (E+P $\rightarrow$ EP) can be neglected. The velocity in this initial period is called the initial velocity v_0. The initial velocity for an enzyme catalyzed reaction is obtained from a progress curve, which is a graph of either the increase in product concentration or decrease in substrate concentration over time. The initial velocity is the slope at the origin of a progress curve. [H. Robert Horton et al., 1996]

2.7.2 The Michaelis-Menten Equation

An enzyme-catalyzed reaction can, like any chemical reaction, be described by a mathematical rate equation. Experiments have shown that the shape of a v_0 versus [S] curve from low to high [S] is a rectangular hyperbola, see Figure 2.7.

The equation for the rectangular hyperbola used in enzyme kinetics is the Michaelis-Menten equation, Equation 2.10. This equation is named after Leonor Michaelis and Maud Menten.

$$v_0 = \frac{V_{max}[S]}{K_m + [S]} \tag{2.10}$$

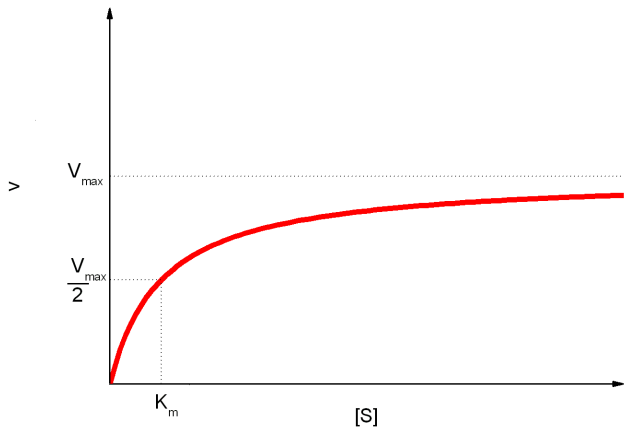

Figure 2.7: Plot of rate velocity v_0 versus substrate concentration [S] for an enzyme-catalyzed reaction. V_{max} is the rate velocity when the substrate concentrations goes to infinity. K_m is equal to the substrate concentration when the initial velocity is one-half of V_{max}

The maximum velocity V_{max} is the value of v_0 for a reaction where E is saturated with S, meaning that all enzymes are occupied by a substrate molecule. K_m is the Michaelis constant, which is defined as the concentration of the substrate when v_0 is equal to one-half of V_{max} .[H. Robert Horton et al., 1996]

2.7.3 Steady-state derivation

The steady-state approximation is often used to verify the Michaelis-Menten equation. The starting point for this derivation is the mixing of E and S. The concentration of S is very high, compared to the concentration of the enzyme, so that it can be considered as constant. The concentration of E begins to drop as the formation of enzyme-substrate complexes starts. The velocity of this formation is given by the rate equation $v = k_1[E][S]$. At the same time as the concentration of ES increases the velocity of the breakdown of ES to E+S and E+P rises. Since the breakdown of ES is via two reactions the velocity for the breakdown is defined as the sum of the velocity for both reactions, v=k$_{-1}$[ES]+k$_{cat}$[ES]. At some point the formation and decomposition of the ES complex will equalize each other and the concentration of the ES complex will remain constant in time. The steady state conditions have now been reached and remain like this until the concentration of substrate approach the concentration of the enzyme, which will not be considered in this approximation. This equilibrium can be expressed as in Equation 2.11.

$$(k_{-1} + k_{cat})[ES] = k_1([E]_{total} - [ES])[S] \tag{2.11}$$

The left side describes the rate of decomposition of the ES complex and the right side describes the rate of formation of the ES complex. This equation can

be rearranged to collect the rate constants on one side and thereby the Michaelis constant K_m can be obtained.

$$\frac{k_{-1} + k_{cat}}{k_1} = K_m = \frac{([E]_{total} - [ES])[S]}{[ES]} \tag{2.12}$$

This equation is now solved for [ES] and gives:

$$[ES] = \frac{[E]_{total}[S]}{K_m + [S]} \tag{2.13}$$

The next step is to utilize the fact that the velocity of an enzymatic reaction is the rate of formation of E+P from ES, which can be expressed as:

$$v = k_{cat}[ES] \tag{2.14}$$

By substituting the value for the [ES] from Equation 2.13 into Equation 2.14 with $v = v_0$ we have:

$$v_0 = \frac{k_{cat}[E]_{total}[S]}{K_m + [S]} \tag{2.15}$$

Since the concentration of the substrate is high compared to the concentration of enzymes it is reasonable to assume that the solution is saturated. This means that an addition of more substrate will not increase the initial velocity of the reaction, only the addition of more enzymes will increase the initial velocity. The maximum velocity V_{max} is defined as the velocity when all the enzymes is present in an enzyme-substrate complex, which can be expressed as:

$$V_{max} = k_{cat}[E]_{total} \tag{2.16}$$

By using the definition of V_{max} it is possible to rewrite the equation into the most familiar form of the Michaelis-Menten equation:

$$v_0 = \frac{V_{max}[S]}{K_m + [S]} \tag{2.17}$$

From this derivation it can be seen that the catalytic constant is equal to V_{max} divided by the total enzyme concentration. k_{cat} represents the number of moles of substrate converted to product under saturated conditions per mole of enzyme. The catalytic constant is therefore a representation of the maximum number of substrate molecules converted into product each second by each active site. In other words, k_{cat} is a measure of how fast a specific enzyme can catalyze a given reaction. The Michaelis constant K_m is defined as the substrate concentration at one-half of V_{max}, which can be verified by substituting $V_{max}/2$ for v_0 in Equation 2.17.

From Equation 2.12 it can be seen that K_m is the ratio of the constants from breakdown of the ES complex and the constant for its formation. If the turnover number is small compared to the two other rate constants, it can be neglected and

K_m becomes k_{-1}/k_1, which is the equilibrium constant for the breakdown of the ES complex into E+S. Therefore K_m is a measure of the enzymes' ability to bind the substrate. Low values of K_m indicate that the enzymes are capable of binding the substrate tightly and vice versa.

Since the K_m value indicates how effective a given enzyme is to bind a specific substrate, it is often used to compare enzymes which catalyze the same reaction. [H. Robert Horton et al., 1996]

2.7.4 Determination of K_m and V_{max}

The two constants K_m and V_{max} can be obtained by measuring the initial velocity at a series of substrate concentrations at a fixed enzyme concentration. The series of substrate concentrations have to be spread out in order to produce a hyperbola. A good rule of thumb is that the series of substrate concentrations have to range from one-fifth of K_M to five times K_M. It is then possible to estimate the two constants by fitting a hyperbola to the obtained results. This fitting is necessary since it is difficult to determine the two constants directly from the experimental result.

Another way of determining the two constants is by rewriting the Michaelis-Menten equation into a form where the two constants can be obtained from a straight line on a graph. There exists more than just one way to do this, but one of the most commonly used transformation is the double-reciprocal, or Lineweaver-Burk, plot, see Figure 2.8.

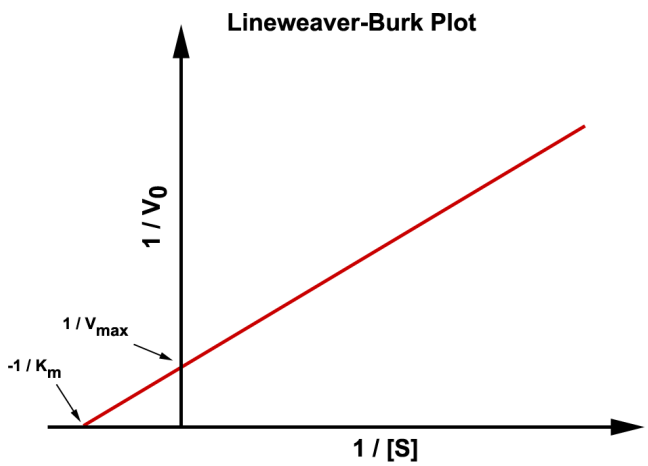

Figure 2.8: Double-reciprocal, or Lineweaver-Burk, plot. $1/v_0$ is plotted as a function of $1/[S]$

In this plot the reciprocal of the velocity is plotted against the reciprocal of the substrate concentration. The mathematical expression for the Lineweaver-Bruk plot

is:

$$\frac{1}{v_0} = \left(\frac{K_m}{V_{max}}\right)\frac{1}{[S]} + \frac{1}{V_{max}} \tag{2.18}$$

This equation is found by taking the reciprocal of Equation 2.10. Plotting the experimental results in this way makes it possible to determine the value of $-1/\mathrm{K}_m$ from the intercept of the line at the x axis and the value of $1/\mathrm{V}_{max}$ from the intercept at the y axis. [H. Robert Horton et al., 1996]

Another type of transformation is the Eadie-Hofstee transformation, which also gives a linearization of the measurements. In this plot the initial velocity is plotted as a function of the initial velocity divided by the substrate concentration. The Eadie-Hofstee plot can be seen in Figure 2.9. V_{max} can be found as the intercept with the y axis and -K_M is equal to the slope of the line.

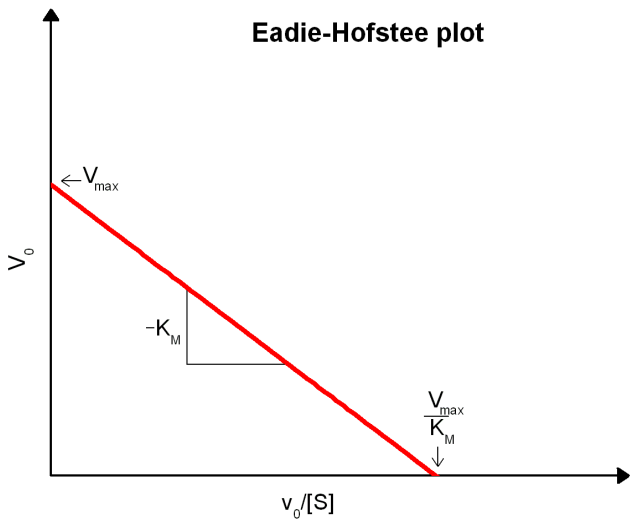

Figure 2.9: Eadie-Hofstee plot. v_0 is plotted as a function of $v_0/[S]$

The equation of the Eadie-Hofstee plot can be found by rearranging Equation 2.10. Equation 2.10 is first inverted, multiplied with V_{max} and then v_0 is isolated. The final equation looks like:

$$v_0 = -K_M\frac{v_0}{[S]} + V_{max} \tag{2.19}$$

Another type of linearization of the experimental results is the Hanes-Wolf plot where $[\mathrm{S}]/\mathrm{v}_0$ is plotted as a function of [S]. This type of transformation will not be used in this report and therefore it will not be treated any further. [Leskovac, 2003]

CHAPTER 3

Materials and Methods

3.1 Production of Colloidal Gold

$HAuCl_4$ was reduced to form solid Au in the production of colloidal gold. Trisodium citrate was used as reduction agent and as a stabilizer. The chemicals and the amounts used can be found in Table 3.1

Chemical	Amount	CAS#
$HAuCl_4$ (Aq) 1 mM	20 mL	16961-25-4
1% $Na_3C_6H_5O_7 \bullet 2H_2O$	2 mL	6132-04-3

Table 3.1: The chemicals and the amounts needed in the production of colloidal gold

The 20 mL of gold ion solution was put in a 50 mL beaker and placed on a heating plate equipped with a magnetic stirrer. At the boiling point the trisodium citrate was added and the solution was boiled until it turned clear red. The produced nanoparticles was placed in the fridge until use.

3.2 Procedure of Immobilization

This procedure describes how the proteins were immobilized on the gold and polystyrene nanoparticles.

The immobilization on gold nanoparticles was done using the two linkers 11-mercaptoundecanoic acid (11-MUDA) and 16-mercaptohexadecanoic acid (16-MHDA).

The polystyrene nanoparticles at 40 nm (Lot. 30198) and 510 nm (Lot. 30517) was purchased with linkers and the procedure for protein immobilization on these will therefore only include Section 3.2.2.

3.2.1 Attachment of Linkers

The chemicals used in the attachment of the linkers can be found in Table 3.2. The 10 mM Na_3PO_4 buffer was prepared using 1.64 g of Na_3PO_4 (CAS# 7601-54-9) and adjusting the volume to one liter and the pH to 7.

Chemical	Concentration	CAS#
Na_3PO_4 buffer pH 7	10 mM	7601-54-9
Colloidal gold solution	-	-
11-MUDA C_2H_5OH solution	5 mM	73768-94-2
16-MHDA C_2H_5OH solution	5 mM	69839-68-5
Tween 20	-	9005-64-5

Table 3.2: The chemicals used in the attachment of the linkers

1 mL of gold particles and 1 mL of Na_3PO_4 buffer with Tween 20 was mixed and left for 30 minutes. In the case of 16-MHDA the Tween 20 concentration was 1.65 μL/mL and 82.5 μL/mL in the case of 11-MUDA. 1 mL linker solution was added after the 30 minutes and the solution was left for 3 hours. Now the excess linker was removed by centrifugation at 16,000 g for 30 minutes. This was done three times and after each cycle the supernatant was removed and the particles resuspended in an equal amount of Na_3PO_4 buffer. The first two times the buffer contained Tween 20. The third time the particles were resuspended in pure buffer. In the case of the 16-MHDA linker the first resuspension was carried out using 99.9% C_2H_5OH instead of buffer as this linker was poorly soluble in water.

3.2.2 Activation of Carboxylic Groups and The Immobilization of Proteins

The chemicals used in the activation of the carboxylic groups and the immobilization of the proteins can be found in Table 3.3

Chemical	Concentration	CAS#
Na_3PO_4 buffer pH 7	10 mM	7601-54-9
EDC solution	160 mM	1892-57-5
NHS solution	160 mM	6066-82-6
Cutinase solution	$\approx$ 1 mg/mL	-

Table 3.3: The chemicals used to activate the carboxyl groups and immobilize the enzymes

Equal amounts of freshly prepared EDC and NHS solutions were mixed and 3 μL/mL was added to the gold nanoparticle solution and left for 30 minutes. In the

case of polystyrene nanoparticles was 3 μL/mL of the EDC and NHS solution was mixed with 1 mL of polystyrene particle solution and 1 mL of Na_3PO_4 buffer and left for 30 minutes. The polystyrene nanoparticle stock solution was diluted 1:100 before use.

Now the solutions were centrifuged one time at 16,000 g for 30 minutes, the supernatant was removed and the particles resuspended in pure buffer.

10 μL cutinase solution was added and the solutions were again left for 30 minutes.
Afterwards the solution was centrifuged three times for 30 minutes at 10,000 g and after each cycle resuspension was carried out using pure buffer.

3.2.3 Localized Surface Plasmon Resonance

LSPR was measured in order to ensure that the linkers and linkers with proteins was attached to the gold nanoparticles. It was done using UV1 spectrometer from Thermo Electron Corporation (serial: uv124716).

An absorbance scan between 400 nm and 650 nm was taken of the following samples; pure gold nanoparticles, gold nanoparticles with linkers, and gold nanoparticles with linker and cutinase.

3.3 Determining the Secondary Structure

In order to determine if the secondary structure of cutinase was changed by the immobilization process circular dichroism was used. The apparatus used was Jasco-J715 (serial: Bo19460524). A constant temperature scan was carried out at wavelengths between 190 nm and 300 nm. Measurements was carried out on cutinase stock and on gold samples with cutinase immobilized on the surface.

The two samples containing gold was concentrated by centrifugation at 10,000 g for 30 minutes and then resuspended in 1/3 of the original volume. The measurements was carried out using a cuvette with a path length of 0.1 mm. More information about the method of CD can be found in Appendix B

3.4 Measurement of Size

3.4.1 AFM

AFM was used to determine the size of the pure gold particles and gold particles with linker and proteins. The instrument used was a Multimode^{TM} Atomic Force Microscope.

Before the size of the particles could be measured they had to be immobilized on a silicon wafer. The following steps explain how the immobilization was performed.

The silicon wafers were first cleaned in an ultrasonic bath for 15 minutes. Absolute ethanol was used as the solvent in the ultrasonic bath. After this cleaning process, the silicon wafers were submerged into a 3% 3-aminopropyltriethoxysilane (APTES, CAS# 9019-30-2) solution for 30 minutes. The silicon wafers were then gently rinsed with absolute ethanol two times and one time with MiliQ water. When the silicon wafers had been rinsed, it was possible to immobilize the particles on the surface of the silicon wafers.

This immobilization was performed by adding 30 μL of the desired sample on a silicon wafer. From this point two approaches were used, one where the droplet stayed for two hours and one where it stayed for 10 minutes. After the time period, the sample was gently rinsed with MiliQ water and then dried with a flow of nitrogen. The finished sample could now be analyzed with the atomic force microscope. More information about the immobilization can be found in Appendix A.

3.4.2 Dynamic Light Scattering

The size distribution of the different gold nanoparticle solutions were measured with DLS using DynaPro 99 (serial: 99-57).

1 mL of the following solutions was measured; pure gold nanoparticles, gold nanoparticles with linkers, and gold nanoparticles with linkers and protein.

3.5 Activity of Cutinase

In order to test the activity of cutinase p-Nitrophenylbutyrate (p-NPB) was used as substrate. The chemicals used to prepare the p-NPB stock solution can be found in Table 3.4. When cleaved by cutinase into p-NP and butyric acid the p-NP part colors the solution yellow. The development of this color change was monitored using a spectrophotometer set at 420 nm. It should be mentioned that p-NP is colorless at pH below 5.6 but this should not cause any problems in the activity test since the Tris HCl buffer has pH 7.5. The 50 mM Tris HCl buffer was prepared by dissolving 7.88 g of solid Tris HCl (CAS# 1185-53-1) in MiliQ water and adjusting the volume to one liter and the pH to 7.5 using HCl.

Chemical	Amount	CAS#
p-NPB	8.2 μL	2635-84-9
C_2H_5OH 99.9%	91.8 μL	-

Table 3.4: The chemicals used to prepare the p-NPB stock solution

When running the test 1 mL cuvettes were used and the amount of chemicals listed in Table 3.5 were added to the cuvette.

As reference a cuvette was prepared without cutinase and the volume was adjusted to 1 mL using 50 mM Tris pH 7.5.

Chemical	Amount
50 mM Tris HCl pH 7.5	985 μL
1 μg/mL Cutinase solution	5 μL
0.5 M p-NPB C_2H_5OH solution	10 μL

Table 3.5: The amount of chemical added to a 1 mL cuvette during activity tests

The spectrophotometer was set to record a scan with 30 second intervals over a period of 30 minutes. Just before starting the scan the p-NPB was added to the cuvettes.

The amount of p-NP, produced by the enzymes in the cuvette, can by calculated from the absorbance curve via Beer-Lamberts law. The extinction coefficient for p-NP is equal to 3.89 mLμmol^{-1}cm^{-1}.

3.5.1 Determination of V_{max}, K_M, and k_{cat}

In order to determine the values of V_{max}, K_M, and k_{cat} another activity test was performed. This time it was a dilution of the cutinase stock solution, 1:100, which was tested. The difference between the earlier described activity test and this one was the amount of substrate added to the cuvettes. The amount p-NPB was ranging from 0.5 μL to 35 μL of the p-NPB stock solution.

CHAPTER 4

Results

4.1 Localized Surface Plasmon Resonance

In this section the results from the measurements of the localized surfade plasmon resonance peaks are presented. The LSPR measurements have been made to ensure that the linker and the protein are actually attached to the gold nanoparticles. Attachment of linker and protein should produce a red shifting of the LSPR peak due to changes in the local environment of the nanoparticle.

4.1.1 Linker 16-MHDA

Figure 4.1 shows the results obtained using 16-MHDA as linker. The LSPR peak of pure gold nanoparticles is positioned at 523 nm, a bit higher than expected. This can be attributed to the citrate molecules which are linked to the nanoparticles to stabilize them because they too produce a change in the local environment. This means that the change in LSPR peak from pure gold to gold and linker will not be as apparent as one might first expect, because the overall change in local environment from pure gold to gold with linker is not just equal to the change caused by the linker. Even due to this, the red shift is from 523 nm to 526 nm. This change can only be attributed to the presence of linker on the gold nanoparticles.

The red shift in LSPR peak when cutinase is attached to the linker is from 526 nm to 530 nm. It would be reasonable to suppose that the shift should be smaller than the shift from pure gold to gold with linker because the change occurs farther away from the gold particle, and thus does not produce a change as local as the attachment of linker. Cutinase however, is a much larger molecule than the linker so it produces a measurable change even though it is not situated immediately next to the gold particle. The red shift of the peak indicates that some proteins are

attached to the linker and it can with fair reliability be concluded that the proteins are attached to the gold particles through the linker.

The reduction in intensity of the peaks is due to the centrifugation process where some gold particles are unavoidably removed each cycle.

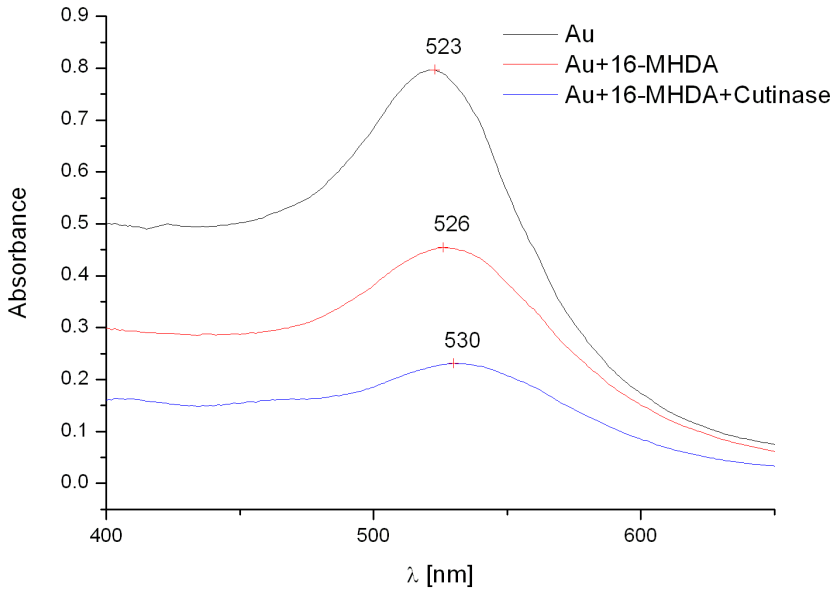

Figure 4.1: Absorbance measurements of pure gold particles, gold particles with linker attached and gold particles with linker and protein. The linker was 16-MHDA. The peak is due to LSPR and the peak red shifts as the thickness of the dielectric layer increases on the nanoparticle.

4.1.2 Linker 11-MUDA

Figure 4.2 shows the results obtained using 11-MUDA as linker. Here too a change in the absorbance peak is expected when the linker is attached. It is seen that the change is smaller than when using 16-MHDA as linker. This can be explained by the fact that 11-MUDA is a smaller molecule and therefore does not produce as large a change.

When cutinase is attached to the linker the LSPR peak changes from 525 nm to 530 nm. This change is a bit larger than the change when using 16-MHDA. Again, this can be attributed to the 11-MUDA linker being shorter than the 16-MHDA so that the large cutinase molecules get closer to the gold particles.

As with the 16-MHDA linker, it is clear that measurable changes occur when linker and protein are attached to the gold particles. These results are good evidence that the proteins are actually attached to the gold particles.

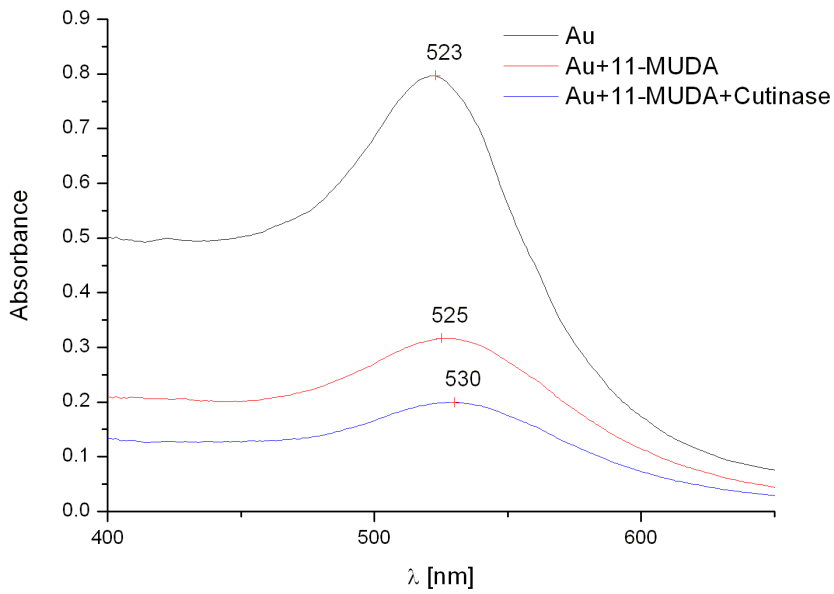

Figure 4.2: Absorbance measurements of pure gold particles, gold particles with linker attached and gold particles with linker and protein. The linker was 11-MUDA. The peak is due to LSPR and the peak red shifts as the thickness of the dielectric layer increases on the nanoparticle.

4.2 Measurements of Size Distribution

This section will present the results from AFM and DLS in order to verify the size distribution of the gold nanoparticles with and without linker and protein.

4.2.1 AFM

Figure 4.3 is the result from the AFM images of gold nanoparticles. Figure 4.3(a) shows that the particles are well separated and the height on Figure 4.3(c) gives a diameter of 13-15 nm.

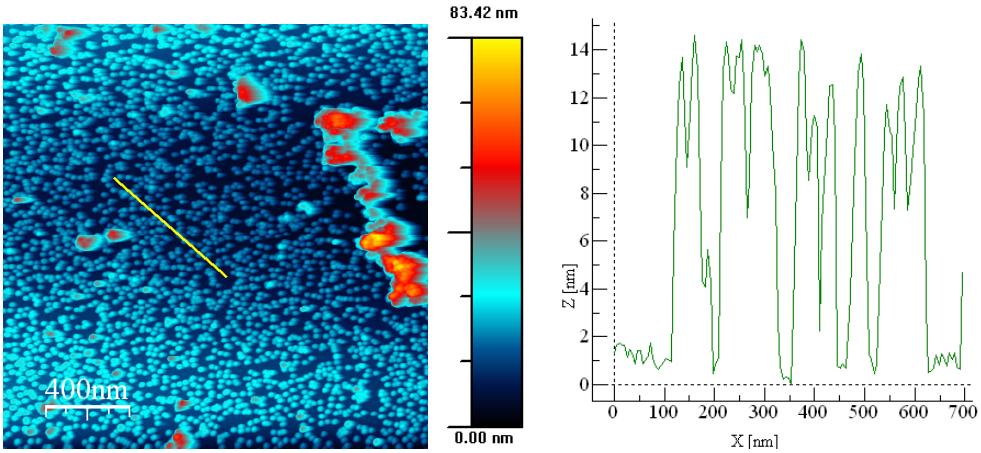

(a) (b) (c)

Figure 4.3: (a) is a 2-D scan of colloidal gold, (b) is the scale bar of the height, and (c) is a roughness analysis of the scan indicated by the yellow line on (a). The height on (c) is 13-15 nm and this is also the diameter of the particles.

Figure 4.4 is the result from the AFM images of gold nanoparticles with 11-MUDA and cutinase. Figure 4.4(a) shows that the particles are less separated than pure gold nanoparticles. This could be caused by the proteins denaturing on the gold nanoparticles and therefore making them more inclined to aggregation. Another explanation could be that more gold nanoparticles will bind to the same enzyme due to the number of primary amines exposed on the surface of cutinase. The height on Figure 4.4(c) gives a diameter of 13-16 nm.

Figure 4.5 is the result from the AFM images of gold nanoparticles with 16-MHDA and cutinase. Figure 4.5(a) shows that the particles are less separated than pure gold nanoparticles and the explanation is the same as above. The height on Figure 4.5(c) gives a diameter of 15-18 nm.

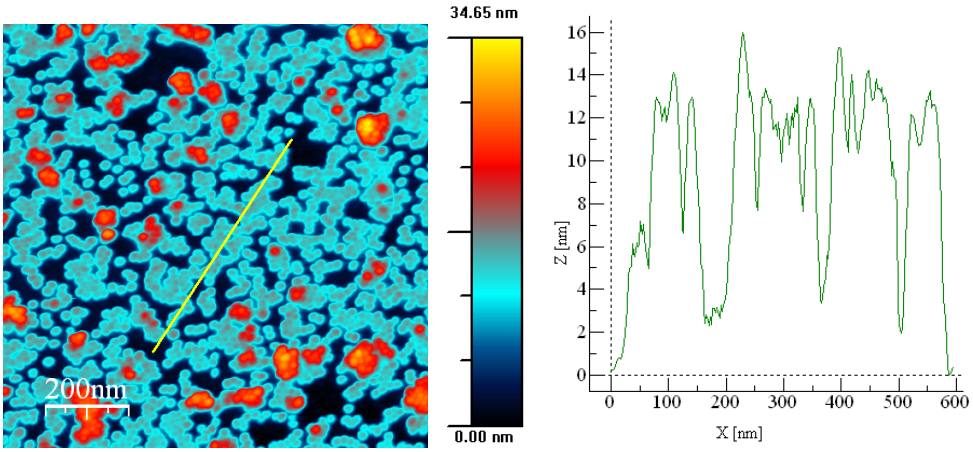

(a) (b) (c)

Figure 4.4: (a) is a 2-D scan of colloidal gold with 11-MUDA and cutinase, (b) is the scale bar of the height, and (c) is a roughness analysis of the scan indicated by the yellow line on (a). The height on (c) is 13-16 nm and this is also the diameter of the particles with linker and enzyme.

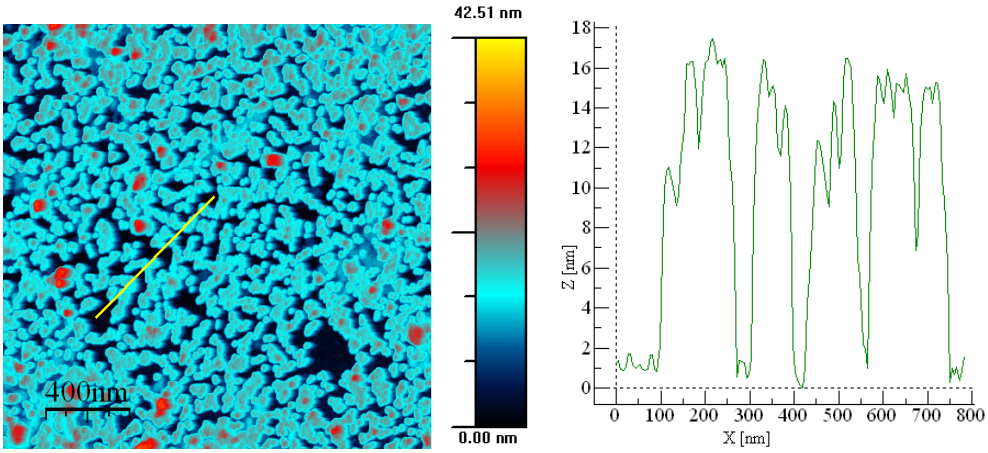

(a) (b) (c)

Figure 4.5: (a) is a 2-D scan of colloidal gold with 16-MHDA and cutinase, (b) is the scale bar of the height, and (c) is a roughness analysis of the scan indicated by the yellow line on (a). The height on (c) is 15-18 nm and this is also the diameter of the particles with linker and enzyme.

4.2.2 Dynamic Light Scattering

The size distribution measure using DLS can be seen in Table 4.1.

It is seen that the average radius of pure gold nanoparticles is 8 nm. It increases to around 14 nm when the linkers are attached and to around 19 nm when cutinase is attached. It is therefore reasonable to assume that both linkers and cutinase are attached to the gold nanoparticles.

The DLS measurements on pure gold nanoparticles show an average diameter of around 16 nm and the AFM images show a diameter of around 14 nm. However, a rather large size difference between DLS and AFM occurs when the linker and linker plus protein are attached. The AFM images show that some of the particles are aggregated and some are not. This could explain why DLS measures a larger average diameter. This could also explain why the deviation in DLS increases when linker and cutinase are attached as both small and large particles will be present in the solution.

Sample	Average Radius [nm]	Deviation [nm]
Au	8.01	1.75
Au with 11-MUDA	14.21	5.62
Au with 11-MUDA and Cutinase	19.22	9.01
Au with 16-MHDA	14.73	5.90
Au with 16-MHDA and Cutinase	19.52	7.16

Table 4.1: DLS measurements of pure gold particles, gold particles with linker, and gold particles with linker and cutinase. 11-MUDA and 16-MHDA were used as linkers. The average radius and the deviation from this average radius is given for each type of particles.

4.3 Circular Dichroism

In order to determine if the structure of the immobilized proteins are changed as a result of the proximity to the gold particles circular dichroism was used. In this section the CD data is presented.

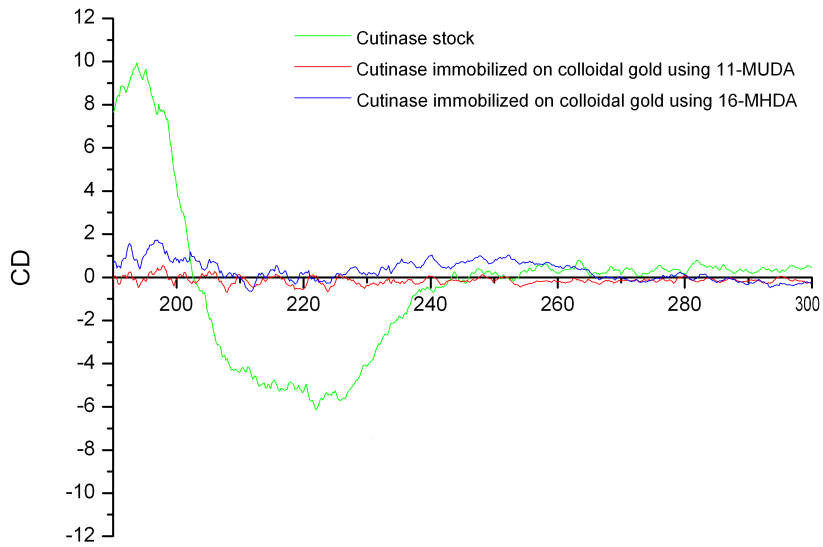

Figure 4.6: Circular dichroism spectroscopy of cutinase stock solution (green) and cutinase immobilized on colloidal gold using 11-MUDA (red) and 16-MHDA (blue).

The green line in Figure 4.6 shows the data of the cutinase stock solution. From the data it is evident that there are secondary structure present in the proteins.

The red and blue lines in Figure 4.6 show the circular dichroism scan of protein immobilized on gold nanoparticles using 11-MUDA and 16-MHDA as linkers respectively. There are two possible ways of interpreting these data. Either the proteins are denatured as a result of the proximity to the colloidal gold or more likely the concentration of protein is too small to measure any secondary structure using CD.

4.4 Calculation of Enzyme Concentration

The concentration of enzyme can be calculated using the law of Lambert-Beer as described in Section 2.5. Because small amounts of enzyme is used, it is difficult to accurately measure the weight. It is often easier and more precise to add some reasonable amount of enzyme to the solution, measure the absorbance at 280 nm and calculate the concentration. The exact wanted concentration can then be obtained by dilution.

The absorbance of the cutinase stock solution was measured and the result can be seen in Figure 4.7. It shows an absorbtion of 0.619 at 279 nm. Using the calculated molar absorption coefficient of 14690 M^{-1} cm^{-1} (Section 2.5) the concentration turns out to be:

$$c = \frac{A}{\epsilon_{280} l} \rightarrow c = 0.042 \mu mol/ml \tag{4.1}$$

It was the intention to measure the enzyme absorbance after immobilization on gold nanoparticles, but when measuring the enzyme absorbance after immobilization the picture is quite different. The absorbance peak at 280 nm is for all practical purposes not present, which makes it impossible to determine the enzyme concentration after immobilization to any reasonable accuracy. The concentration will be calculated from the enzyme kinetics experiments in Section 4.6

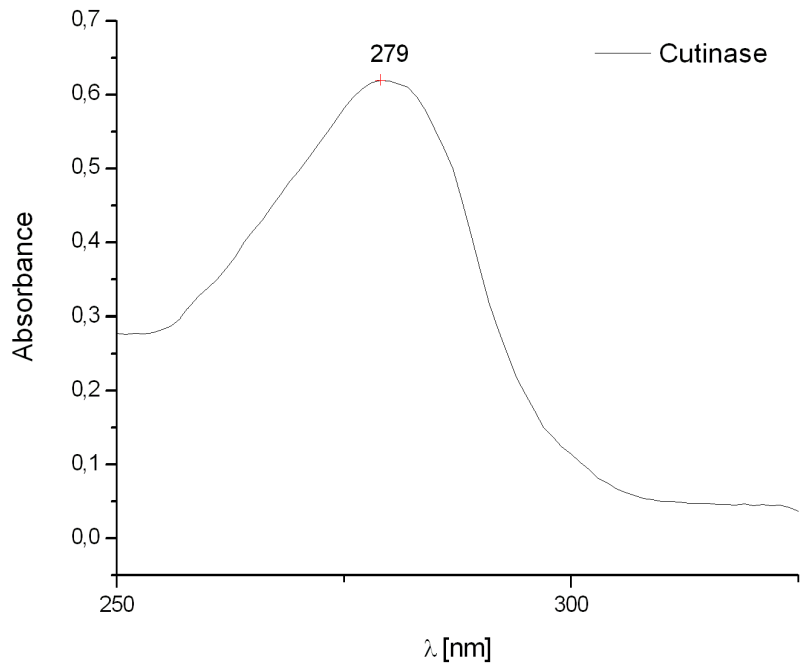

Figure 4.7: Absorbance spectrum of cutinase. The peak is at 279 nm and the maximal absorption is 0.619.

4.5 Effect of Centrifugation

The gold and polystyrene solutions where centrifuged three times after attachment of protein in order to remove any non-immobilized proteins from the solutions. Enzyme activity was measured after each cycle and this section will present these results.

4.5.1 Gold Nanoparticles with 11-MUDA

Figure 4.8(a) is the results from enzyme activity using gold nanoparticles with 11-MUDA as linker and Figure 4.8(b) is the absorbance spectra taken after each centrifugation. In Figure 4.8(c) the drop in activity of immobilized enzymes per centrifugation is compared with the drop in concentration of gold per centrifugation.

From Figure 4.8(a) it is evident that the enzyme activity is significantly lower after each centrifugation. The difference in the first and second centrifugation indicates that non-immobilized proteins are removed. A third centrifugation was conducted to ensure that all non-immobilized proteins were removed. The result however showed a further drop in enzyme activity. This result may indicate that not all excess protein was removed by the second centrifugation.

Another explanation to the drop in the enzyme activity could be that some of the gold nanoparticles with immobilized protein are removed after each centrifugation. Figure 4.8(b) confirms this assumption. These results show that the drop in activity after each centrifugation is also caused by the removal of gold nanoparticles with immobilized proteins, because the intensity of the absorption from gold drops too. A calculated time for the sedimentation of the gold particles with linker and protein can be found in Appendix C. This time was found to be 17 minutes. Because the centrifugation time was 30 minutes this indicates that all gold particles should be centrifuged down. However, the results show that gold is still present in the supernatant.

Figure 4.8(c) have been made in order to make it easier to compare the drop in enzyme activity with the drop in gold concentration after each centrifugation. The enzyme activity and gold concentration is set to 100 % after the first centrifugation. It can be seen that the slope of the enzyme activity curve from the first to the second centrifugation is greater than the slope of the gold concentrations curve. This may indicate that the lowering in the enzyme activity is partially caused by the removal of non-immobilized enzymes and partially by the removal of gold nanoparticles with immobilized enzymes.

The slopes of the enzyme activity and gold concentration curves are more similar between the second and third centrifugation compared with the slopes between the first and second centrifugation. The lowering in the enzyme activity may be ascribed mainly to the lowering in the gold concentrations. This means that the concentration of non-immobilized enzymes is decreasing after each centrifugation, which was the purpose with the centrifugation. In the ideal experiments the slope of the two curves would be equal to each other, as the drop in activity would be directly proportional to the drop in gold particle concentration.

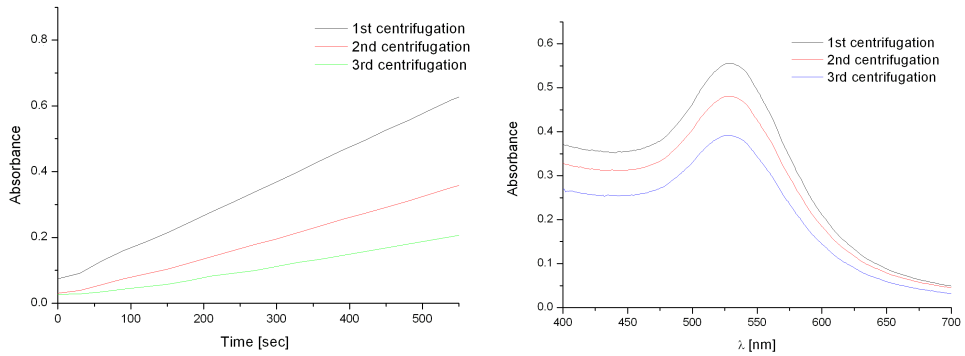

(a)

(b)

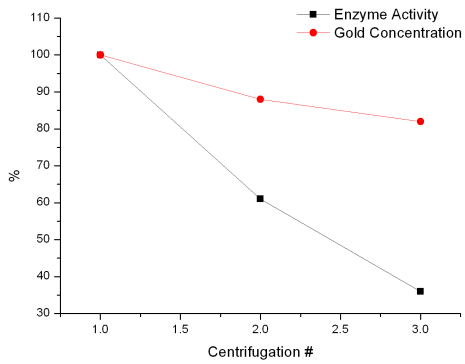

(c)

Figure 4.8: Results from activity test (a) and absorbance spectra (b) of gold nanoparticles with 11-MUDA as linker. (c) is the drop in activity of immobilized enzymes compared to drop in concentration of gold nanoparticles, which both are a function of the number of centrifugations. The results obtained after the first centrifugation are set to 100 %.

4.5.2 Gold Nanoparticles with 16-MHDA

The results from enzyme activity using 16-MHDA as linker on gold nanoparticles is shown in Figure 4.9(a) and the absorbance spectra after each centrifugation is shown on Figure 4.9(b). Figure 4.9(c) compare the drop in the enzyme activity of immobilized enzymes per centrifugation with the drop in concentration of gold per centrifugation.

The results from Figure 4.9(a) shows that the enzyme activity is lower for each centrifugation and Figure 4.9(b) confirms that gold nanoparticles are removed after each centrifugation. Figure 4.9(c) indicate that the decrease in the enzyme activity between the first and second centrifugation is a consequence of the removal of non-immobilized enzymes and the removal of gold nanoparticles with immobilized enzymes. The decrease in the enzyme activity from the second to the third centrifugation is probably only a consequence of the lowering in the gold concentration,

since the slope of the two curves is similar.

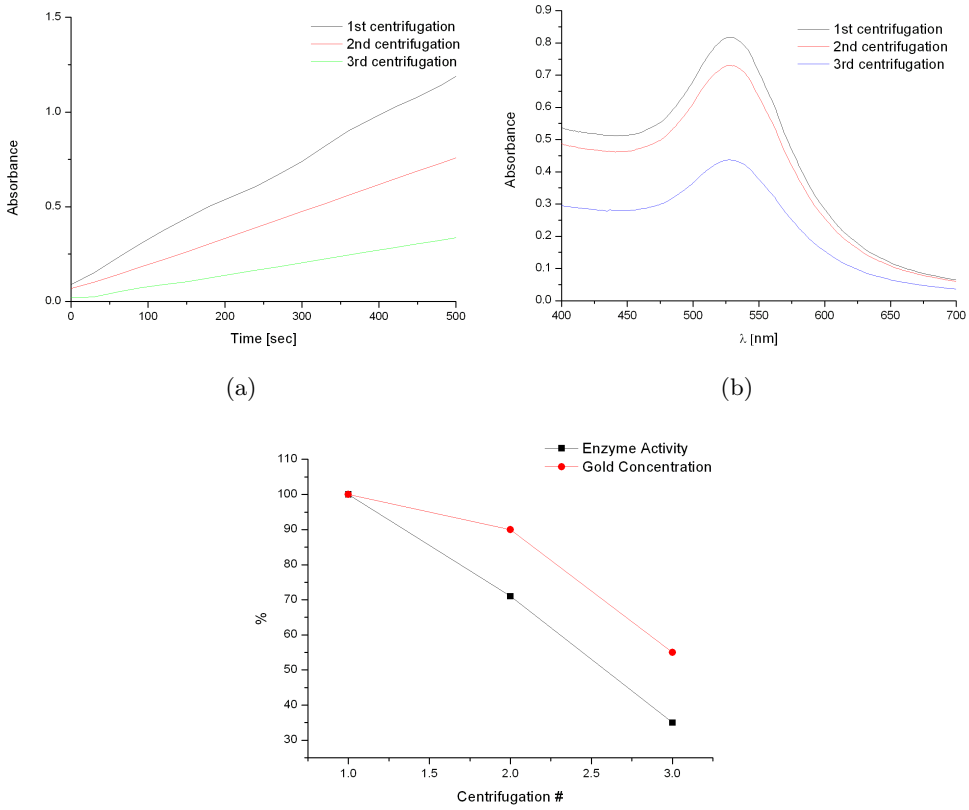

Figure 4.9: Results from activity test (a) and absorbance spectra (b) of gold nanoparticles with 16-MHDA as linker. (c) is the drop in activity of immobilized enzymes compared to drop in concentration of gold nanoparticles, which both are a function of the number of centrifugations. The results obtained after the first centrifugation are set to 100 %.

4.5.3 40 nm Polystyrene Nanoparticles

Polystyrene nanoparticles with a diameter of 40 nm was used and the result is seen in Figure 4.10. The large drop in enzyme activity can be explained by the fact that almost all polystyrene nanoparticles are removed after the second centrifugation. This is actually not a surprising result because of the particles being almost impossible to centrifuge down. The pellet could not be seen with the naked eye and it was therefore difficult to remove the supernatant without also removing most of the polystyrene particles. The density of polystyrene (1050 kg/m^3) is much lower than that of gold (19300 kg/m^3) and this explains why polystyrene nanoparticles was so much more difficult to centrifuge down than gold nanoparticles. In order to

determine if these particles needed more time to reach the bottom, a calculation on the time needed was performed. The calculation can be found in Appendix C. The time was found to be 35 hours under centrifugation of 10,000 g, which may explain the large drop in activity after centrifugation.

Another, but less likely, reason could be that the proteins are not immobilized on the polystyrene particles. However if this was the case then the proteins should have been separated in the firs centrifugation and the activity results contradict this assumption.

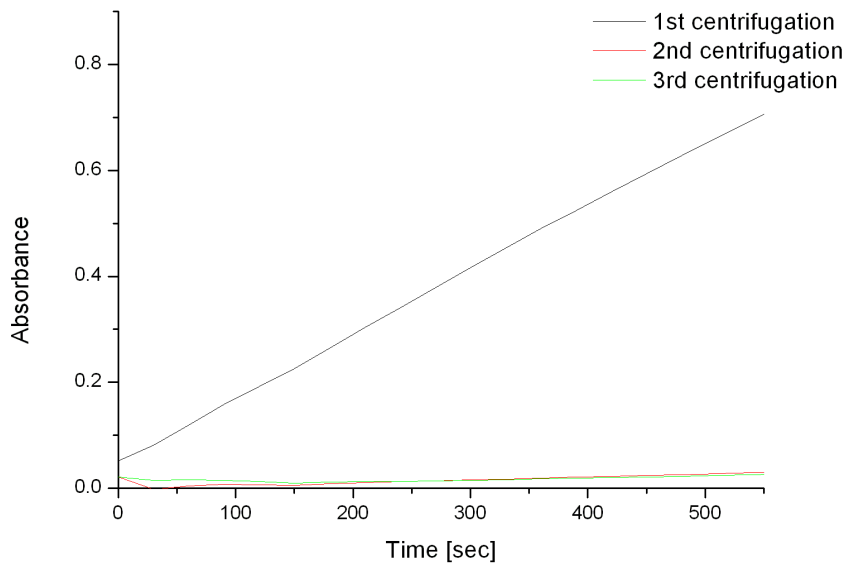

Figure 4.10: Results from activity test of polystyrene nanoparticles with a diameter of 40 nm.

4.5.4 510 nm Polystyrene Nanoparticles

The results from polystyrene nanoparticles with a diameter of 510 nm are shown in Figure 4.11. There is almost no difference in activity after centrifugation, indicating that all excess protein is removed by the first centrifugation. The first centrifugation result actually seems to have the lowest enzyme activity but this can be explained by a small error in the amount of stock solution added to the activity test. A calculated time for the sedimentation of the 510 nm polystyrene particles can be found in Appendix C. The time was calculated to be 5.43 minutes, which is better than for the gold nanoparticles. This explains the small drop in activity after centrifugation of 510 nm polystyrene particles.

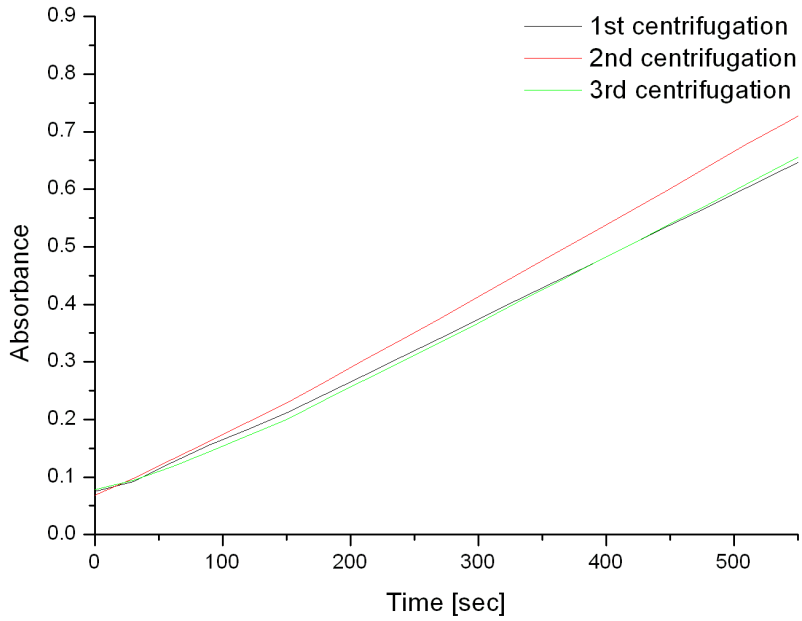

Figure 4.11: Results from activity test of polystyrene nanoparticles with a diameter of 510 nm.

4.6 Enzyme Kinetics

This section will present the results obtained from the kinetic analysis of cutinase. These results are used to calculate the values of V_{max} and K_M in the experiments and k_{cat}. The turnover number is finally used to estimate the enzyme concentration in the samples where cutinase have been immobilized on gold and polystyrene particles.

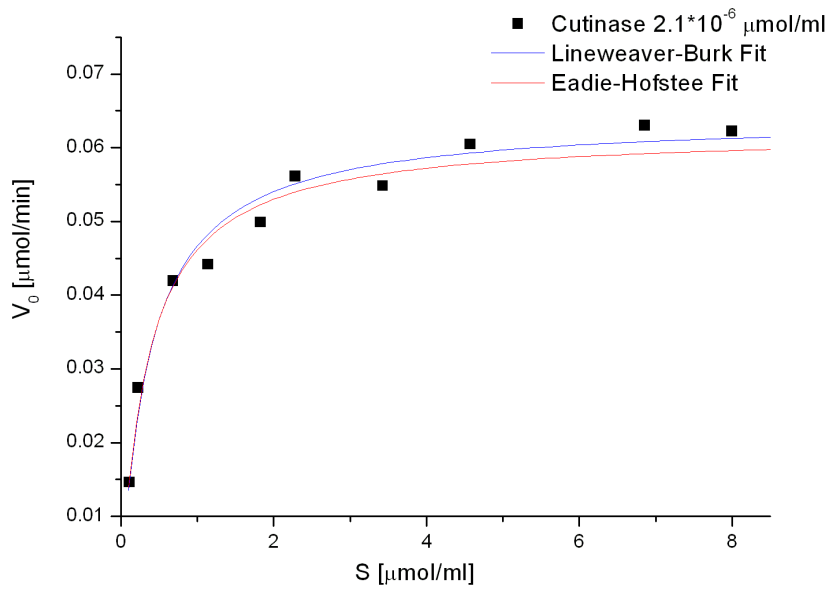

Figure 4.12: The black squares show the measured values of the initial velocity at different substrate concentrations. The enzyme concentrations are held fixed at $2.1 \cdot 10^{-6} \mu mol/mL$. *The blue curve is a hyperbola fit, which is found via the Lineweaver-Burk plot. The red curve is a hyperbola fit, which is found via the Eadie-Hofstee plot.*

Figure 4.12 shows the initial velocities measured as a function of the substrate concentration. As it can be seen the initial velocity is measured at ten different substrate concentrations ranging from 0.1 mM to 8.0 mM. The concentration of cutinase is held fixed at $2.1 \cdot 10^{-3} \mu$M in all the experiments.

It can been seen that the plot of the measurements form a hyperbola shape which makes it possible to calculate the three constants, which also means that the choice of substrate concentrations is suitable.

The equation for the blue hyperbola curve is found through the Lineweaver-Burk plot, which can be seen in Figure 4.13. From the plot it can be seen that lack of accuracy when preparing the experiment with low substrate concentrations is of great importance. It will affect the slope of the linear fit in a stronger way than errors in the preparation of experiments with high substrate concentrations. Therefore the problem with this type of linearization of the experimental data is that the initial velocities at different substrate concentrations are not equally weighted.

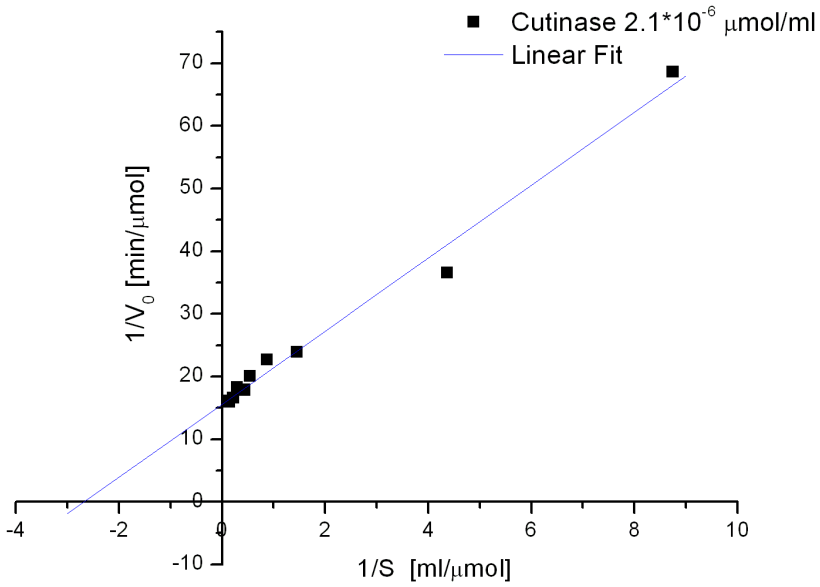

Figure 4.13: Lineweaver-Burk plot. Values of $1/v_0$ are plotted as a function of 1/[S]. The black squares shows the measured values and the blue curve is a linear fit of the measurements.

The equation for the red hyperbola is found via the Eadie-Hofstee plot, which can be seen in Figure 4.14. The initial velocity is plotted as a function of the initial velocity divided by the substrate concentration. It can be seen that this type of linearization is not affected by errors in experiments with low substrate concentrations in the same way as the Lineweveaver-Burk plot. The measured values are more spread out in the Eadie-Hofstee plot compared to the Lineweveaver-Burk plot. In spite of this advantage, this type of linaerization also have a weakness. When an error is made in the measurement of the initial velocity it will affect both axes, which is not the case in the Lineweveaver-Burk plot. This is the reason why both types of plots are made.

The values for K_M and V_{max} can easily be found from the equation of the linear fit as described in Section 2.7. The calculated constants from the Lineweveaver-Burk and the Eadie-Hofstee plot are listed in Table 4.2. In order to calculate the turnover number Equation 2.16 has to be used. The turnover numbers are also presented in Table 4.2. In an article written by [H. Chahinian et al., 2005] similar turnover number for cutinase catalyzed breakdown of p-NPB was found. [H. Chahinian et al., 2005] have measured the turnover number to be 31500 min^{-1}.

As it can be seen in the three figures, there are mismatches between the values from the experiments and the fitted curves. The fact that the product, from the enzyme catalyzed reaction, p-NP reached its solubility before V_{max} was reached may be one of the reasons for the mismatches. The problem with the solubility could be solved in two ways. One way is to dilute the cutinase stock solution, which

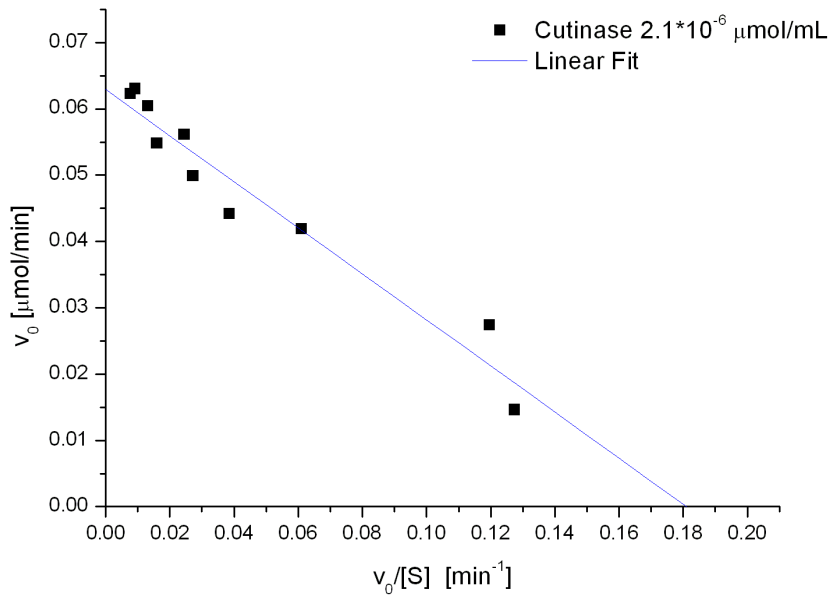

Figure 4.14: Eadie-Hofstee plot. Values v_0 are plotted as a function of $v_0/[S]$. The black squares shows the measured values and the blue curve is a linear fit of the measurements.

Constants	Lineweaver-Burk	Eadie-Hofstee
V_{max}	0.0644 μmol/min	0.0622 μmol/min
K_M	0.374 μmol	0.347 μmol
k_{cat}	30544 min^{-1}	29957 min^{-1}

Table 4.2: shows the calculated values of V_{max}, K_M, and k_{cat}. The constants have been calculated from both the Lineweawer-Burk and Eadie-Hofstee plot.

mean a lower substrate concentration is needed in order to reach the maximum initial velocity. Another way to solve the problem is by stirring in the cuvettes in between the measurements. The first one was not chosen since the amount of product produced by the enzymes will then give a very low absorbance. The last one was therefore chosen and due to this choice it was not possible to make measurements within short intervals, which may have affected the measurements.

4.6.1 Estimation of Cutinase Concentration after Centrifugation

The turnover numbers found via the Lineweaver-Burk and the Eadie-Hofstee plot have been used to estimate the concentrations of cutinase in the different samples after they have been centrifuged three times.

The calculated concentrations of the immobilized cutinase can be seen in Table 4.3. It can be seen that the immobilization of cutinase on polystyrene nanoparticles

with a diameter of 510 nm has been the most successful one and that the use of 16-MHDA as linker gives a better results in preference to the used of 11-MUDA. The immobilization of cutinase on polystyrene nanoparticles with a diameter of 40 nm did not succeed and therefore no concentration has been calculated.

Sample	Enzyme Conc. (L-B)	Enzyme Conc. (E-H)
Au with 11-MUDA	$1.88 \cdot 10^{-4}$ μM	$1.92 \cdot 10^{-4}$ μM
Au with 16-MHDA	$3.20 \cdot 10^{-4} \mu$M	$3.26 \cdot 10^{-4}$ μM
Polystyrene 40 nm	–	–
Polystyrene 510 nm	$5.81 \cdot 10^{-4}$ μM	$5.92 \cdot 10^{-4}$ μM

Table 4.3: shows the estimated concentration of active cutinase immobilized on gold nanoparticles and polystyrene nanoparticles. The turnover number found via the Lineweaver-Burk plot and the Eadie-Hofstee plot have been used to calculate the values in the column: Enzyme Conc. (L-B) and Enzyme Conc. (E-H) respectively.

CHAPTER 5

Discussion

5.1 Attachment of Linkers

It is a crucial step in the immobilization process that the linkers are attached to the gold nanoparticles. AFM, DLS and LSPR measurements have been made in order to test this step.

From the DLS measurements it is seen that the average size of linker plus nanoparticle solution is larger than the average size of pure nanoparticles by 5 nm. This size increase is seen for both 11-MUDA and 16-MHDA linker. The change can be attributed to the attachment of the linkers on the nanoparticles, increasing their average radius. However, the linkers also form micelles without gold particles within them. This will also affect the DLS measurements because they do not distinguish between micelles with and without gold particles. However, the amount of micelles without gold particles should be minimal after the centrifugation process. If there are micelles present, it could be because the gold particles have been flung out of the micelles during the centrifugation.

The AFM pictures do not show a clear increase of the size of the nanoparticles when the linkers and the proteins are attached. The size increase will be more obvious from the DLS results, because DLS measures the hydrodynamic radius. From the LSPR measurements however, a red shifting in the peak wavelength is seen when the linker is attached. This change is most likely caused by the presence of the linkers on the gold particle surface, because the LSPR peak is not affected by formation of micelles.

5.2 Immobilization of Cutinase

To examine the outcome of the immobilization LSPR, DLS and AFM measurements was made. The absorbance of the sample was also measured in order to determine

the concentration of immobilized enzyme. However, as stated in the results chapter, the 280 nm peak from the enzyme was not present. This can be interpreted in two ways. Either the enzymes are not present on the gold nanoparticles, or present in very small amounts, or the presence of the gold nanoparticles shifts the absorbance peak wavelength to shorter or longer wavelengths. Measuring the absorbance from 190 nm to 900 nm however indicates no shifting of the absorbance peak to neither shorter or longer wavelengths.

The DLS results show an increase in average size from gold with linker to gold with linker and cutinase of 5 nm. This result indicates immobilization of enzymes, but can also be a result of formation of enzyme aggregates in the solution.

Again, LSPR supports the immobilization of enzymes because a shift in the peak wavelength is seen.

Because both the DLS results and the LSPR measurements indicate that the enzymes *are* immobilized on the gold particles, it is reasonable to believe that the reason why the 280 nm peak is so weak is that the enzyme concentration is very low. This hypothesis is also supported by the activity tests after each centrifugation as described in Section 4.5.

It was intended to measure the condition of the immobilized proteins using CD, to determine whether the immobilization process itself or the presence of the gold particle destroys the secondary structure of the protein. However, because the concentration of enzymes after immobilization was too low, it was not possible to get any useful data from CD.

5.3 Enzyme Kinetics

The goal of the activity tests and enzyme kinetics measurements was to measure the activity of cutinase after immobilization on the gold particles, and compare this activity with the activity of the enzyme stock solution. Ideally, this would give an answer to the question whether the presence of nanoparticles inhibits or destroys the enzyme function.

The kinetics measurements on enzyme stock solution gave results comparable to the results obtained in other studies. In this study the k_{cat} number was measured to be approximately 30,000 min^{-1}, which is reasonable compared to other studies.

Measuring the same parameters on the enzymes immobilized on gold nanoparticles showed to be very difficult, because the concentration of enzymes after immobilization is very low.

In the immobilization process 10 μL cutinase stock solution was added, which gave an initial concentration of $4.2 \cdot 10^{-4}$ μmol/mL. Using the results from the activity tests, which was measured after the last centrifugation, the concentration after immobilization is estimated to be between $1.8 \cdot 10^{-7}$ and $5.9 \cdot 10^{-7}$ μmol/mL, which is just about a factor of 1000 lower than the initial concentration. This lowering of the effective enzyme concentration is primarily caused by the centrifugation process, where a large part of the enzymes are removed, but the lowering may also be caused

by other effects such as denaturation of the enzymes during immobilization and inhibition of activity by the gold particles. Even though only such a small part of the initial enzyme population is present after immobilization, activity is still seen in the activity tests.

The results obtained from cutinase immobilized on gold nanoparticles indicated that the best activity is achieved when 16-MHDA is used as linker. This could be a result of the 11-MUDA linker being shorter than the 16-MHDA thereby causing the enzyme activity to drop as a result of the proximity to the nanoparticle. Another option is that the smaller surface area posed by the 11-MUDA linker reduces the number of proteins that can possibly be immobilized on the nanoparticle.

The 510 nm polystyrene particles was easier to separate from the solution than gold particles. It is seen that the loss in activity as a function of number of centrifugations is lower than the loss when using gold nanoparticles. The 40 nm polystyrene particles however, was almost impossible to separate.

It is important to be aware that the calculated concentrations of cutinase in the different samples are based on the activity test. Therefore they only give an estimate of the concentration of enzymes. It is reasonable to believe that the amount of immobilized enzymes is higher than the calculated concentrations. Some enzymes may have lost their enzymatic properties in the immobilization process which will contribute to the lowering of the enzyme concentration in the activity tests. The loss in enzymatic properties could be a result of changes in the tertiary structure when the enzymes are immobilized on the nanoparticles. Another possibility is that a primary amine close to the active cite have made a bond to a linker. In this case the active cite will be facing against the nanoparticle which will make the attachment to a substrate molecule difficult. The calculated concentrations are thus the effective concentration of enzymes i.e. the concentration of active enzymes.

CHAPTER 6

Conclusion

In this project the immobilization of cutinase on gold and polystyrene nanoparticles has been studied. Absorption spectroscopy, DLS, CD, and AFM have been used in order to verify that the immobilization of cutinase on the nanoparticles has succeeded.

The results obtained from the LSPR and DLS measurements did all indicate that immobilization of cutinase on the nanoparticles did succeed. Attachment of linkers to the gold nanoparticles increased the size of the gold nanoparticles and the attachment of cutinase to gold nanoparticles also lead to an increase in the size.

From the activity test and the kinetics analyses it was evident that the best result was obtained when the immobilization was performed on polystyrene nanoparticles with a diameter of 510 nm. When the immobilization was performed on gold nanoparticles two different types of linker was used. The best result was obtained when 16-MHDA was used as linker. The immobilization on polystyrene nanoparticles with a diameter of 40 nm did not succeed.

The low concentration of active enzymes in all the immobilization experiments may be a consequence of the presence of nanoparticles close to the enzymes. CD measurements was made in order to confirm this assumption but no useful measurements was produced.

The calculation of the enzyme concentration after the final centrifugation indicate that only one pro mille of the initial enzyme concentration was retained. Therefore an optimization is needed before this type of immobilization technique can be cost-effective.

APPENDIX A

Immobilization of Particles on Silicon Wafers.

Atomic force microscopy was used to determine the size of the gold particles and the complex where linker and proteins were attached to the particle. In order to perform this analysis an immobilization technique was used to fix the particles on a silicon wafer. This appendix will deal with this immobilization technique in more details and describe how 3-aminopropyltriethoxysilane (APTES) is used in the immobilization process.

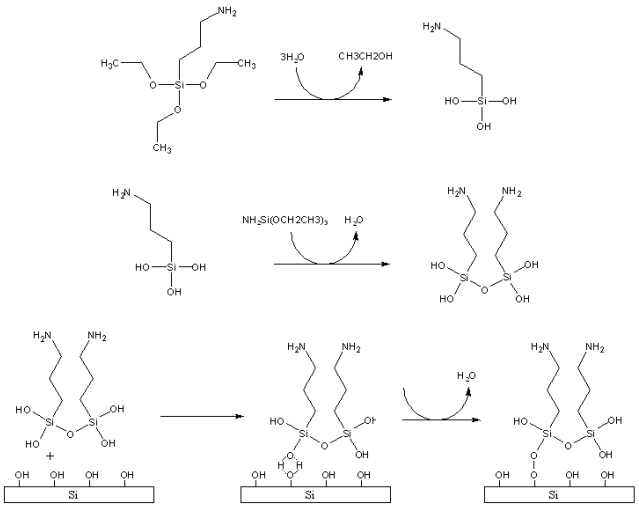

Figure A.1: Flowchart describing the formation of a silane monolayer on a silicon wafer. (Top) hydrolysation of the ethyl group on the three ethoxy chains. (Middle) condensation reaction between two hydrolyzed APTES molecules. (Bottom) condensation reaction between a hydrolyzed APTES molecule and the hydroxylized silica

The starting point of this immobilization is the native silicon wafers. The silicon wafers are covered with an oxide layer, silica, which is formed when the silicon is exposed to air. This native silica layer is hydrolyzed when it comes into contact with water and thereby forms a hydroxide layer. This hydroxide layer is utilized in the attachment of the APTES molecules on the surface of the wafers.

The silanization reaction used in the immobilization of the APTES molecules can be seen in Figure A.1.

The first step is the hydrolysation of the ethyl group on the three ethoxy chains. After this hydrolyzation two paths can be taken. The silane molecule can make a condensation reaction with another silane molecule or with the hydroxylized silica. The reaction with the silica results in the formation of silane monolayer on top of the silica surface, where the amino group on the silane molecules is pointing away from the silica. When these amino groups come into contact whit water, they react with the water and forms positively charged ammonium ions.[A. Simon et al., 2002]

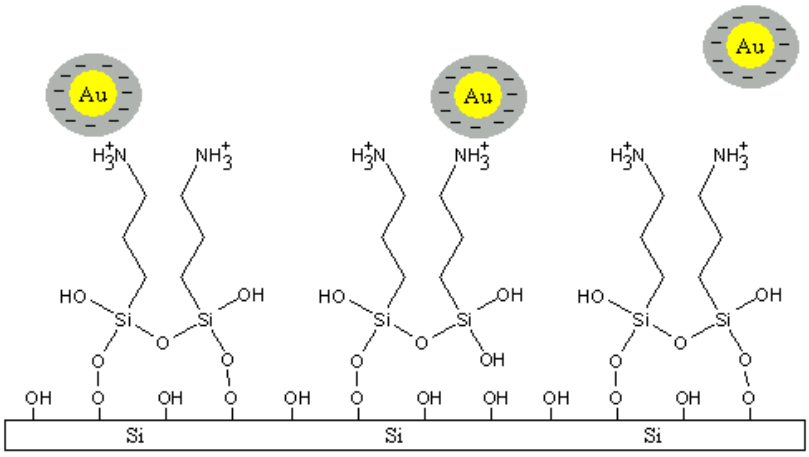

Figure A.2: The deposition of negatively charged gold on the positively charged ammonium ions .

Since the particles of interest are negatively charged when they are contained in there respective solutions they will be attracted by the ammonium ions and form an electrostatic bond, as it can be seen in Figure A.2. This electrostatic bond keeps the particle fixed when the excess solvent and particles are gently rinsed away. The particles are now immobilized and can be analyzed in the atomic force microscope. [S. Liu et al., 2002]

APPENDIX B

Circular Dichroism

Circular dichroism (CD) belongs to the methods of chiroptical spectroscopy which are spectroscopy methods that utilizes circular polarized light. In the case of CD both left and right circular polarized light, (lcp) and (rcp) light respectively, are used. Circular polarized light is composed of two orthogonal plan polarized light waves with a difference in phase of $\pm$ 90° or $\pm$ $\pi/2$ radians. An electric field vector $\overrightarrow{E_{sum}}$ is now defined as the summation of the intensity vectors of the vertical and the horizontal electric fields. The phase shift between these two orthogonal fields causes the tip of $\overrightarrow{E_{sum}}$ to trace out a corkscrew motion. As the beam propagates the electric field vector $\overrightarrow{E_{sum}}$ takes one revolution around the axis of propagation with in one wavelength. It is the corkscrew motion that determine if the light is left or right circular polarized. If the corkscrew motion of rcp light is observed from a receivers perspective the motion of the screw will be clockwise and in the case of lcp light it will be a counterclockwise motion. An illustration of lcp light can be found in Figure B.1. [Fasman, 1996]

Circular dichroism is defined as the difference in absorbtion between lcp and rcp light at different wavelengths. In order for the CD to work the molecules that are being examined must be chiral meaning that the molecule is antisymmetric in the sense that it can not cover its own mirror image like a left and a right hand not being able to cover one another while having the same side turned upwards. The word dichroism means having two colors which is exactly the case for chiral molecules as the absorbance depends on which polarization they are illuminated with.[Fasman, 1996]

The absorbtion of light is described by Lambert-Beers law and applied to lcp light it yields as follows

$$\Delta A = -\log_{10}\left(\frac{I_l}{I_l^0}\right) = \varepsilon_l C L \tag{B.1}$$

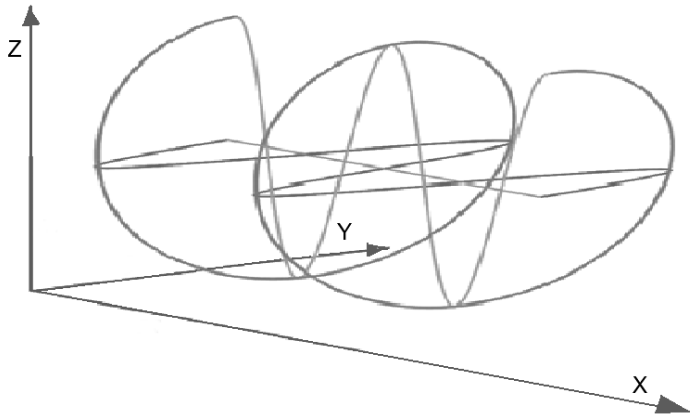

Figure B.1: Illustration of left circular polarized light the direction of propagation is in x. modified from [www.jchemed.chem.wisc.edu, 2006]

where I_l^0 is the intensity of the lcp light illuminating the sample and I_l is the intensity reaching the detector. ε_l is the decadic molar extinction coefficient of the chiral solute for lcp light, C is the molar concentration of the solute and L is the path length of the cuvette. [Fasman, 1996]

A similar expression can be defined for rcp light. Combing this with Equation B.1 following expression yields

$$\Delta A = A_l - A_r = \varepsilon_l CL - \varepsilon_r CL = \Delta\varepsilon CL \tag{B.2}$$

From Equation B.2 $\Delta\varepsilon$ can be found and used to report CD data.

The original method of measuring CD was by illuminating the sample with plan polarized light. Plan polarized light is a superposition of two light waves of equal field intensity, one lcp and one rcp. As this is send through a dichroic medium the difference in absorbtion of the two components causes the plane polarized light to be transformed into elliptically polarized light, which is also left or right polarized depending on which circular component that is the strongest. Before the plan polarized light interacted with the dichroic medium the phase shifted horizontal components canceled each other out as they are equal in size but opposite in direction causing the $\overrightarrow{E_{sum}}$ vector to oscillate in the vertical plane. The absorbtion of one component weakens the canceling potential and causes $\overrightarrow{E_{sum}}$ to shift from the vertical plane yielding an elliptic corkscrew shape as the wave propagates. This is illustrated on Figure B.2(a).[Fasman, 1996]

The proportions of the ellipse traced out by $\overrightarrow{E_{sum}}$ can be used to report CD data. This is done using the relation ship between half the minor and half the major radius of the ellipse. The relationship is $\tan(\theta)$ and is called the ellipticity. This angle is in

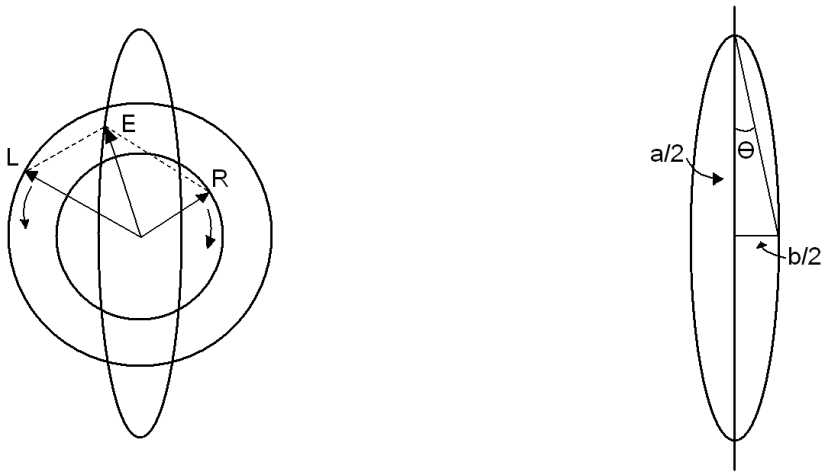

(a) (b)

Figure B.2: Figure B.2(a) illustrates how absorbtion of rcp component of plan polarized light cause the electric field vector to trace out an elliptic shape. As the two vectors L and R are pointing in the same direction the combined electric field vector defines the major radius of the ellipse and as L and R are pointing in opposite direction the minor radius of the ellipse is defined. Figure B.2(b) illustrates the parameters used to report CD data. θ is the angle defined by half of the extremal axis of the ellipse where a/2 is the major and b/2 is the minor radius. Modified from [Fasman, 1996]

general very small and can therefore be approximated by angle θ in radians. Figure B.2(b) illustrates this relationship.

$$\theta \approx \tan(\theta) = \frac{\left(|\overrightarrow{E}_l| - |\overrightarrow{E}_r|\right)}{\left(|\overrightarrow{E}_l| + |\overrightarrow{E}_r|\right)} \tag{B.3}$$

By expressing the electric fields of Equation B.3 as oscillating exponential functions controlled by the absorbtion A_l and A_r and by converting to degrees the following appears

$$\theta(\text{deg}) = 32.98 \cdot \Delta A \tag{B.4}$$

From this it is evident that the ellipticity is directly proportional to the CD. To remove the linear dependance of concentration and path length a molar ellipticity is defined as

$$[\theta] = \frac{100 \cdot \theta}{CL} \tag{B.5}$$

by inserting Equation B.2 and Equation B.4 into Equation B.5 the following yields

$$[\theta] = 3298\Delta\varepsilon \tag{B.6}$$

From this expression it can be seen that the relation ship between molar ellipticity and $\Delta\varepsilon$ is linear. But as a result of history CD data is normally reported in terms of variation in molar ellipticity as a function of wavelength. [Fasman, 1996]

APPENDIX C

Centrifugation

The centrifugation was carried out to separate the particles from the solution. Sedimentation theory was used in order to determine the time needed to separate the particles from the solution.

General Formulas and Theory

A particle of mass m suspended in a medium has the effective mass

$$m_e = m \cdot b \tag{C.1}$$

where b accounts for buoyancy and is defined as

$$b = 1 - \rho \cdot \nu_s \tag{C.2}$$

ρ is the density of the solvent and ν_s is the partial specific volume of the particle meaning the volume of solvent that one gram of the material displaces. The unit of ν_s is $[mL/g]$.[Atkins and Paula, 2006]

If the solution is placed in a centrifuge and set to spin with an angular velocity ω in a distance r from the center of rotation the particle will experience a centrifugal force which is described by the following equation.[Atkins and Paula, 2006]

$$F_c = m_e \cdot r \cdot \omega^2 \tag{C.3}$$

Furthermore the particle will experience a frictional force arising from the molecules in the solvent. This friction is proportional to the particles drift speed s and defined as follows:

$$F_f = s \cdot f \tag{C.4}$$

Where f is the frictional coefficient defined as $f = 6\pi a\eta$ for spherical particles where a is the radius of the particle and η is the viscosity of the solvent. This force causes the particle to drift with a constant speed in the solution only depending on the external force F_c.[Atkins and Paula, 2006]

Below is an expression for the force the centrifuge must develop in order to get the particle traveling with a certain speed.

$$F_c = s \cdot f \tag{C.5}$$

From this expression it is possible to calculate the time t needed to travel a certain distance d. Meaning that it is possible to calculate when the particle will reach the bottom of the tube. An expression for this follows.

$$t = \frac{d}{s} \tag{C.6}$$

By rearranging and isolating s in Equation C.5 and inserting in Equation C.6 following expression yields.

$$t = \frac{f \cdot d}{F_c} \tag{C.7}$$

Newtons second law provides that $F_c = m_e a_c$ by substituting this into Equation C.7 and inserting the values for f the following yields.

$$t = \frac{6\pi a\eta \cdot d}{m_e a_c} \tag{C.8}$$

Where a_c is the centripetal acceleration of the centrifuge.

Calculation of Sedimentation Time for a 40 nm Polystyrene Particle

The following example calculates the time needed to make a 40 nm polystyrene particle travel a distance of 2.5 centimeter under the influence of an acceleration of 10,000 g.

The first thing is to calculate the volume of such a particle. This is done as follows

$$V = \frac{4}{3}\pi a^3 = \frac{4}{3}\pi(20 \cdot 10^{-9})^3 = 3.351 \cdot 10^{-23} m^3 \tag{C.9}$$

The density of polystyrene is 1050 kg/m^3 which gives the particle a mass of

$$m = 1050\frac{kg}{m^3} \cdot 3.351 \cdot 10^{-23} m^3 = 3.5186 \cdot 10^{-20} kg \tag{C.10}$$

Now the b factor is calculated using the density ρ of water and the partial specific volume of polystyrene.

$$b = 1 - \rho \cdot \nu_s = 1 - 1 \cdot g/mL \frac{1}{1.050 g/mL} = 0.0385 \tag{C.11}$$

$$m_e = m \cdot b = 3.5186 \cdot 10^{-20} kg \cdot 0.0385 = 1.3533 \cdot 10^{-21} kg \tag{C.12}$$

Using the viscosity of water $\eta = 0.000891 \frac{kg}{m \cdot s}$ and inserting the numbers in Equation C.8 the following yields.

$$t_{40nm} = \frac{6\pi 20 \cdot 10^{-9} m \cdot 0.000891 \frac{kg}{m \cdot s} \cdot 0.025 m}{1.3533 \cdot 10^{-21} kg \cdot 10,000 \cdot 9.82 \frac{m}{s^2}} = 126378 s \approx 35 hours \tag{C.13}$$

This result indicates that it would be advantages to use a higher acceleration to retrieve these particles from an aqueous solution.

Sedimentation Calculations for the Remanning Particles

The time needed for a 510 nm polystyrene particle to travel 2.5 centimeter under the influence of 10,000g

$$t_{510nm} = 326 s \approx 5 minutes and 26 seconds \tag{C.14}$$

The time needed for a 16 nm gold particle with linker and protein to travel 2.5 centimeter under the influence of 10,000g. The linkers and proteins make the particle appear to have a size of 19.52 nm. The size is found via DLS.

$$t_{19.52nm} = 1063 s \approx 17 minutes and 43 seconds \tag{C.15}$$

BIBLIOGRAPHY

[A. Simon et al., 2002] A. Simon, T. Cohen-Bouhacina, M. C. Porté, J. P. Aimé, and C. Baquey (2002). Study of two grafting methodes for obtaining a 3-aminopropyltriethoxysilane monolayer on silica surface. *Journal of Colloid and Interface Science*.

[Atkins and Paula, 2006] Atkins, P. and Paula, J. (2006). *Physical Chemistry*. Oxford.

[C. N. Pace et al., 1995] C. N. Pace, F. Vajdos, L. Fee, G. Grimsley, and T. Gray (1995). How to measure and predict the molar absorption coefficient of a protein. *Protein Science*.

[Catherine Soanes et al., 2006] Catherine Soanes, Sara Hawker, and Julia Elliott (2006). *Oxford English Dictionary Sixth Edition*. Oxford University Press.

[Creighton, 1993] Creighton, T. E. (1993). *Proteins - Structures and Molecular Properties*.

[D. M. Schulz and A. Sinz, 2004] D. M. Schulz and A. Sinz (2004). Chemisches cross-linking und massenspektrometrie zur strukturellen und funktionellen charakterisierung von proteinen. *BIOspektrum*.

[Eggins, 2006] Eggins, B. R. (2006). *Chemical Sensors and Biosensors*. Wiley.

[Fasman, 1996] Fasman, G. D. (1996). *Circular Dichroism and the Conformational Analysis of Biomolecules*. Plenum Press.

[G. A. Macedo and T. F. Pio, 2005] G. A. Macedo and T. F. Pio (2005). A rapid screening method for cutinase producing mircoorganisms. *Brazillian Journal of Microbiology*.

[H. Chahinian et al., 2005] H. Chahinian, Y. Ben Ali, A. Abousalham, S. Petry, L. Mandrich, G. Manco, S. Canaan, and L. Sarda (2005). Substrate specificity and kinetic properties of enzymes belonging to the hormone-sensitive lipase family: Comparison with non-lipolytic and lipolytic carboxylesterases. *Science Direct*.

[H. Robert Horton et al., 1996] H. Robert Horton, Laurence A. Moran, Raymond S. Ochs, J. David Rawn, and K. Gray Scrimgeor (1996). *Principles of Biochemistry*. Prentic-Hall, Inc.

[K. Aslan and V. H. Pérez-Luna, 2002] K. Aslan and V. H. Pérez-Luna (2002). Surface modification of colloidal gold by chemisorption of alkanethiols in the presence of a nonionic surfactant. *Langmuir*.

[Kittel, 2005] Kittel, C. (2005). *Introduction to Solid State Physics*. Wiley.

[Leskovac, 2003] Leskovac, V. (2003). *Comprehensive Enzyme Kinetics*. Kluwer Academic/Plenum Publisher.

[M. Himmelhaus and TH. Takei, 2002] M. Himmelhaus and TH. Takei (2002). Self-assembly of polystyrene nano particles into patterns of random-close-packed monolayers via chemically induced adsorption. *The Owner Societies*.

[S. Liu et al., 2003] S. Liu, D. Leech, and H. Ju (2003). Application of colloidal gold in protein immobilization, electron transfer, and biosensing. *Marcel Dekker*.

[S. Liu et al., 2002] S. Liu, T. Zhu, R. Hu, and Z. Liu (2002). Evaporation-induced self-assembly of gold nanoparticles into a highly organized two-dimensional array. *PCCP*.

[Vadgama, 2005] Vadgama, P. (2005). *Surfaces and Interface for Bio-Materials*.

[www.fu berlin.de, 2006] www.fu berlin.de (2006). Reduction of gold by trisodium citrat. `http://www.diss.fu-berlin.de/2001/54/Kapitel5.pdf`.

[www.jchemed.chem.wisc.edu, 2006] www.jchemed.chem.wisc.edu (2006). Circular polarized light. `http://jchemed.chem.wisc.edu/JCEDLib/SymMath/collection/article.php?id=44`.

[www.lsbu.ac.uk, 2006] www.lsbu.ac.uk (2006). Enzyme reactors. `http://www.lsbu.ac.uk/biology/enztech/reactors.html#fig5_1`.

[www.piercenet.com, 2006] www.piercenet.com (2006). Activation of carboxyl groups. `http://www.piercenet.com/Objects/View.cfm?type=ProductFamily&ID=02030312`.

[www.rcsb.org, 2006] www.rcsb.org (2006). Rcsb protein data bank. `http://www.rcsb.org/pdb/files/1cex.pdb`.

[www.wikipedia.org/Polystyrene, 2006] www.wikipedia.org/Polystyrene (2006). Wikipedia polystyrene. http://en.wikipedia.org/wiki/Polystyrene.

[www.wikipedia.org/Thiol, 2006] www.wikipedia.org/Thiol (2006). Wikipedia thiol. http://en.wikipedia.org/wiki/Thiol.